ARMY RESEARCH LABORATORY

Flight Motion of a Continuously Elastic Finned Missile

by Charles H. Murphy and William H. Mermagen

ARL-TR-2754 June 2002

The findings in this report are not to be construed as an official Department of the Army position unless so designated by other authorized documents.

Citation of manufacturer's or trade names does not constitute an official endorsement or approval of the use thereof.

Destroy this report when it is no longer needed. Do not return it to the originator.

Army Research Laboratory
Aberdeen Proving Ground, MD 21005-5069

ARL-TR-2754 **June 2002**

Flight Motion of a Continuously Elastic Finned Missile

Charles H. Murphy and William H. Mermagen
Weapons and Materials Research Directorate, ARL

Abstract

The motion of elastic finned projectiles has been analyzed by various approximate theories. In this report the exact equations of small amplitude motion are derived for a symmetric missile. The aerodynamic and elastic symmetries are used to allow the use of complex variables to describe the lateral motion in a non-rotating coordinate system. Although the resulting equations are both ordinary and partial differential equations, frequencies and damping rates of free oscillations are obtained from an ordinary differential equation with boundary conditions. Equations for a permanently deformed bent missile are derived, and an ordinary differential equation for the forced motion of a bent missile is obtained. Sample calculations for a finned projectile with a fineness ratio of 20 show resonant motion at the aerodynamic frequency as well as at each elastic frequency. The nonlinear roll moment associated with a bent missile is computed and the location of possible spin-yaw lock-in is determined. The flight motion of an elastic missile is shown to be the sum of two elliptical motions: a low frequency pitching motion and a higher frequency flexing motion. The induced drag coefficients for both motions are computed as functions of the missile's elasticity.

Contents

List of Figures v

List of Tables vii

1. Introduction 1

2. The Coordinate System 2

3. Center of Mass Motion 3

4. Angular Motion of the Projectile 6

5. Flexing Motion of the Projectile 10

6. Bent Missile 13

7. Trim Solution 15

8. Transient Solutions 18

9. Flight Motion 20

10. Induced Drag 21

11. Numerical Results 23

12. Summary 25

13. References 33

Appendix A. Integrals 35

Appendix B. Functions 37

Appendix C. Relationship Between Boundary Conditions 39

Appendix D. Trim Solution Parameters 43

Appendix E. Transient Solution Parameters 45

Appendix F. Missile Parameters 47

List of Symbols 49

Report Documentation Page 53

List of Figures

Figure 1. Sketch of finned missile. 25

Figure 2. $\dot{\phi}_1/\omega_R$ vs. σ for flare-stabilized rod. 26

Figure 3. $\dot{\phi}_1/\omega_R$ vs. σ for finned missile. 26

Figure 4. $\dot{\phi}_3/\omega_1, \dot{\phi}_5/\omega_2$ vs. σ for finned missile. 27

Figure 5. $|\psi_{k2}|$ vs. σ for k = 1, 3, 5. 27

Figure 6. $R\{\psi_k(x)/\psi_{k2}\}$ vs. x for $\sigma = 5$, k = 1, 3, 5. 28

Figure 7. λ_k/ω_R vs. σ for k = 1, 3, 5 28

Figure 8. λ_1/ω_R vs. p/ω_R for $\sigma = 5, \hat{k} = 0, 0.05, 0.10$ 29

Figure 9. $C_l/C_{N\alpha}$ vs. σ 29

Figure 10. $\hat{C}_k$ vs. σ for k = 3, 5. 30

Figure 11. $|\xi_T/\xi_{TR0}|$ vs. p/ω_R for bent finned missile at $\sigma = 5$ 30

Figure 12. $|\delta_E(x_2)/\xi_{TR0}|$ vs. p/ω_R at $\sigma = 5$ for bent finned missile. 31

Figure 13. f_j vs. p/ω_R for bent finned missile at $\sigma = 5$ 31

INTENTIONALLY LEFT BLANK.

List of Tables

Table 1. Values of A_{k0}, N_{k0}, z_{z0} 32

INTENTIONALLY LEFT BLANK.

1. Introduction

Modern antitank kinetic energy projectiles have become very long finned missiles carrying very dense metal rods. Because these projectiles have to resist very large aerodynamic loads due to their high-velocity flight at sea level, designers have been concerned about the possibility of aeroelastic deformations [1–7]. There is some evidence that a small number of these projectiles have been forced to spin at rates close to their lowest elastic frequency and have been subject to large inelastic deformations. Mikhail [3, 4] and Murphy and Mermagen [6, 7] have developed special solutions that showed spin lock-in at the lowest elastic frequency.

Mikhail [3, 4] used an incorrect expression for the angular momentum and assumed erroneously that a spinning elastic missile could perform planar-flexing motion and a planar-pitching motion in a coordinate system rotating with the missile. His numerical calculations, however, showed examples of spin lock-in when fin damage produces a roll-inducing moment sufficient to cause a steady-state spin greater than the lowest elastic frequency, and initial spin was zero. Heddadj et al. [5] approximated an elastic missile by two rigid bodies elastically connected and studied the transient motion of these bodies but did not consider spin lock-in.

Murphy and Mermagen [6, 7] approximated the continuously elastic missile by three rigid bodies connected by two massless elastic beams and derived differential equations of motion for this three-body system. The equations showed that it is impossible to cause spin lock-in by roll inducing moment and zero initial spin alone. Murphy [8, 9] showed that the combination of an offset center of mass (cm) and a trim pitch moment creates a nonlinear roll moment that can produce spin-lock-in at the aerodynamic frequency. The rear beam of the 3-body theoretical model was given an inelastic lateral deformation and spin lock-in at the lowest elastic frequency was observed.

Because Mikhail's [3, 4] approximate equations are far from being theoretically correct, their results can be dismissed. Murphy and Mermagen's [6, 7] equations are valid, but the use of the 3-body model is a major simplification of the actual physical problem. It is the purpose of this report to derive the correct equations for a continuously elastic symmetric projectile. This derivation exploits the missile's aerodynamic and elastic symmetry by describing the transverse motion with complex variables and using a nonrotating coordinate system with its much simpler equations of motion.

Although the resulting equations form a combination of ordinary and partial differential equations containing integrals of the elastic deformation, free

oscillations and constant-spin trim motion of a bent missile can be computed from fourth-order ordinary differential equations. Induced drag for various free oscillations are deduced as quadratic functions of their amplitude. Quadratic roll moments associated with a bent missile are formulated for trim motion, and equilibrium spins that could cause spin-pitch lock-in are located. Numerical integration of the complete set of partial and ordinary differential equations for varying spin would be necessary to verify the actual occurrence of lock-in. Murphy and Mermagen's 3-body theory [6, 7] would, however, be a good indicator of this lock-in behavior.

2. The Coordinate System

If we consider a symmetric missile with no elastic flexing, we can define a non-spinning coordinate system with origin at the rigid missile's cm and X-axis directed along the axis of symmetry. The Z-axis is perpendicular to the X-axis and initially downward pointing, whereas the Y-axis is determined by the right hand rule.

The elastic missile is assumed to consist of a very heavy elastic circular rod of diameter, d, and fineness ratio, L, embedded in a very light symmetric aerodynamic outer structure that may be longer than the rod. We will conceptually slice the missile into a large number of thin disks perpendicular to the X-axis with thickness, dx. For the elastic rod, an elastic nonspinning coordinate system is defined so that its origin at the center of the central disk and the X-axis is tangent to the rod at this point. When the rod flexes, the disks shift laterally perpendicular to the X-axis and cant to be perpendicular to the centerline of the disks.

The angular velocity of the central disk in these nonspinning coordinates is defined to be the vector,

$$\vec{\omega} = (p, q, r). \tag{1}$$

Because the coordinate system pitches and yaws with the missile but does not spin, its angular velocity vector is

$$\vec{\Omega} = (0, q, r). \tag{2}$$

A dimensionless vector specifies the location of the displaced center of a disk at X with respect to the origin of the elastic coordinate system.

$$\vec{\delta}_E(X,\ t) = (X, Y, Z)d^{-1} = (x, \delta_{Ey}, \delta_{Ez}). \tag{3}$$

Because of the mass and aerodynamic symmetry, it is convenient to represent transverse displacements, transverse velocities, transverse angles, and transverse

angular velocities by complex quantities. The transverse disk displacement and the transverse angular velocity, for example, are

$$\delta_E = \delta_{Ey} + i\delta_{Ez}, \qquad Q = q + ir. \tag{4}$$

The lateral location of the cm of the flexing elastic missile can be expressed in terms of the missile's local mass density $\rho_m(x,y,z)$,

$$\delta_c(t) = (d/m)\int \delta_E(x,t)\rho_1(x)dx, \tag{5}$$

where

$\rho_1(X) = d^2 \iint \rho_m(x,y,z)dydz$, and

$m = d\int \rho_1(x)dx$.

Finally, the transverse location of the center of a disk relative to the elastic projectile's cm is

$$\begin{aligned}\delta(x,t) &= \delta_E - \delta_c, \\ &= \delta_y + i\delta_z.\end{aligned} \tag{6}$$

The location of the center of a disk relative to the cm and its velocity relative to the cm are specified by the vectors,

$$\vec{\delta}_{dc} = (x, \delta_y, \delta_z), \tag{7}$$

$$\vec{V}_{dc}\, d^{-1} = (0, \dot{\delta}_y, \dot{\delta}_z) + \vec{\Omega} x \vec{\delta}_{dc}. \tag{8}$$

The transverse components of this relative velocity vector can be written in the form

$$v_{dcy} + iv_{dcz} = (\dot{\delta} - ixQ)d, \tag{9}$$

where

$$\dot{\delta}(x,t) = \frac{\partial \delta}{\partial t}.$$

3. Center of Mass Motion

The velocity of a disk is

$$\vec{V}_d = \vec{V}_c + \vec{V}_{dc}, \tag{10}$$

where

$\vec{V}_c = (v_x.v_y, v_z)$ is the velocity of the cm.

The angle of attack, α, and the angle of sideslip, β, are defined at the central disk for the elastic missile. If the transverse velocity components for this disk are

$$(v_{Ey}, v_{Ez}),$$

$$v_{Ey} + iv_{Ez} = V\xi, \tag{11}$$

where

$\xi = \beta + i\alpha$, and

$V \cong V_E = \left|\vec{V}_E\right| \cong v_x$.

The transverse velocity for cm of the elastic missile is

$$v_y + iv_z = V\xi + \dot{\delta}_c d. \tag{12}$$

The sum of equations (9) and (12) is, therefore, the transverse velocity of a disk.

$$\begin{aligned} v_{dy} + iv_{dz} &= V\xi + \dot{\delta}_c d + (\dot{\delta} - ixQ)d, \\ &= V\xi + (\dot{\delta}_E - ixQ)d. \end{aligned} \tag{13}$$

The aerodynamic force acting on a rigid projectile is assumed to be proportional to ξ and Q and their derivatives. For an elastic missile, a local aerodynamic force needs to be defined in a similar manner. The x coordinate of a point on the rod axis lies between $x_1 = -L/2$ and $x_2 = L/2$. The aerodynamic structure incasing the rod can have a nose windshield of length $x_{23}d$ and its fins could extend beyond the end of the rod by the distance $x_{01}d$. Thus the aerodynamic force is exerted from $x_0 = x_1 - x_{01}$ to $x_3 = x_2 + x_{23}$. If we assume the aerodynamic structure to be quite rigid beyond the ends of the rod, then,

$$\delta_E(x,t) = \delta_E(x_1,t) + (x - x_1)\Gamma_1(x_1,t) \quad ; \qquad x_0 \le x \le x_1; \tag{14}$$

$$\delta_E(x,t) = \delta_E(x_2,t) + (x - x_2)\Gamma_2(x_2,t) \quad ; \qquad x_2 \le x \le x_3. \tag{15}$$

The transverse aerodynamic force exerted on a disk located at x will be assumed to have the form appropriate to a pointed slender body [10, 11]. Thus, the force will be proportional to the local angle of attack and its modified time derivative.

$$dF = \frac{\partial F}{\partial x}dx = -g_1\left[c_{f1}\eta + c_{f2}(\dot{\eta} + iQ)(d/V)\right]dx, \tag{16}$$

where

$F = F_y + iF_z$, and

$g_1 = \rho S V^2/2$.

$c_{fn}(x)$ are two normal force distribution coefficients per axial length and η is the local complex angle of attack. The distribution functions derived for Munk's airship theory [10–12] are, for example,

$$c_{f1} = -2\frac{dA}{dx}S^{-1}; \qquad c_{f2} = 2AS^{-1}, \tag{17}$$

where A(x) is the local cross-sectional area.

A general pointed slender body relationship between c_{f1} and c_{f2} is

$$c_{f2} = -\int_{x_3}^{x} c_{f1}dx. \tag{18}$$

In reference [13], computer programs for calculating c_{f1} for finned missiles are given.

The complex angle between the missile's centerline described by $\delta(x,t)$ and the X-axis will be denoted as Γ and is the spatial derivative of δ,

$$\Gamma \equiv \frac{\partial \delta}{\partial x} = \frac{\partial \delta_E}{\partial x}. \tag{19}$$

The local angle of attack is the angle between the velocity vector and the surface of the missile, which is assumed to be parallel to the centerline. Because the complex angle between the velocity vector and the X-axis is given by equation (13), the following equation results:

$$\eta = \xi + \left(\dot{\delta}_E - ixQ\right)d/V - \Gamma. \tag{20}$$

Equation (20) can be differentiated and the small angular acceleration terms in $\ddot{\delta}$ and $\dot{Q}$ neglected to yield a relation for $\dot{\eta}$

$$\dot{\eta} = \dot{\xi} - \dot{\Gamma}. \tag{21}$$

The total transverse aerodynamic force acting on the missile can be obtained by integrating equation (16) from x_0 to x_3.

$$F = -g_1\left[C_{N\alpha}\xi + C_{N\dot{\alpha}}\left(\dot{\xi}d/V\right) + iC_{Nq}\left(Qd/V\right) - J_1(t) - \dot{J}_2(t)(d/V)\right], \tag{22}$$

where C_{Nj} are listed in Appendix A, $J_j(t)$ are listed in Appendix B.

The axial aerodynamic force is directed along the X-axis and can be approximated by use of an axial drag coefficient per length and a base-pressure drag coefficient c_{Dbp},

$$F_x = -g_1 C_{DX} \cong -g_1 C_D, \tag{23}$$

where

$$C_{DX} = \int_{x_0}^{x_3} c_D(x)dx + c_{Dbp}.$$

The velocity vector of the cm can now be differentiated as

$$\frac{d\vec{V}}{dx} = (\dot{v}_x, \dot{v}_y, \dot{v}_z) + \vec{\Omega} x \vec{V}. \tag{24}$$

The differential equations for the missile's cm are therefore

$$m(\dot{v}_x + qv_z - rv_y) \cong m\dot{V} = -g_1 C_D; \tag{25}$$

$$m(V\dot{\xi} + \dot{V}\xi + \ddot{\delta}_c d - iVQ) = F. \tag{26}$$

Equations (22), (25), and (26) can be combined to yield a simple relation between Q and $\dot{\xi}$. Small terms involving C_{Nq} and $C_{N\dot{\alpha}}$ have been neglected.

$$(V/d)(\dot{\xi} - iQ) = -g_2 C_{L\alpha}\xi + N, \tag{27}$$

where

$C_{L\alpha} = C_{N\alpha} - C_D$,
$g_2 = g_1/md$, and
N is defined in Appendix B.

4. Angular Motion of the Projectile

The transverse aerodynamic moment exerted on the missile is computed with respect to the cm and has contributions from both the transverse aerodynamic force and the axial aerodynamic force.

$$dM = -i(g_1 d)\left[(c_{f1}\eta + c_{f2}(\dot{\eta}d/V))x - c_D\delta\right]dx, \tag{28}$$

where

$M = M_y + iM_z$.

The total transverse aerodynamic moment acting on the projectile can be obtained by integrating equation (28) and adding the base-pressure moment.

$$M = -i(g_1 d)\left[C_{M\alpha}\xi + C_{M\dot{\alpha}}(\dot{\xi}d/V) + iC_{Mq}(Qd/V) - J_3(t) - \dot{J}_4(t)(d/V) - J_5(t)\right], \quad (29)$$

where the C_{Mj} are given in Appendix A.

Each disk pitches and yaws with angular velocity $Q + i\dot{\Gamma}$ and spins with spin rate p_d. The spin angular momentum about the center of a disk is $p_d(d^2/8)dm$ and the transverse angular momentum about the center of a disk is $(Q + i\dot{\Gamma})(d^2/16)dm$. Now the angular momentum of a disk about the cm of the projectile is expressed in the elastic nonspinning coordinate system and the result integrated over all the disks to yield the total angular momentum of the missile. In dynamics terms, we will neglect the mass of the aerodynamic structure and assume ρ_1 to have the constant value of m/Ld. Because spin-yaw lock-in is caused by quadratic terms, quadratic terms are retained in p_d and h_{dx},

$$\vec{H} = (md^2/L)\int_{x_1}^{x_2}(\vec{h}_d + \vec{\delta}_{dc}x\vec{V}_{dc})dx, \quad (30)$$

where

$$p_d = p(1 - \Gamma\bar{\Gamma}/2) + R\{Q\bar{\Gamma}\},$$

$$h_{dx} = [2p(1 - \Gamma\bar{\Gamma}) + R\{(Q - i\dot{\Gamma})\bar{\Gamma}\}]/16, \text{ and}$$

$$h_{dy} + h_{dz} = (Q + i\dot{\Gamma} + 2p\Gamma)/16.$$

Equations (7) and (8) can be employed to yield the three components of the angular momentum vector.

$$H_x = I_x p + md^2 R\{J_7 - Q\bar{J}_6\}; \quad (31)$$

$$H_y + iH_z = I_t Q + imd^2(\dot{J}_6 + J_8), \quad (32)$$

where J_j is defined in Appendix B.

If the missile is assumed to fly at constant pitch angle and its deformed shape is rotating as a rigid body ($Q = 0$, $\dot{\delta} = ip\delta$), the axial angular momentum is

$$H_x = \hat{I}_x p, \quad (33)$$

where

$$\hat{I}_x = I_x + \left(md^2/L\right)\int_{x_1}^{x_2}\left[|\delta|^2 - |\Gamma|^2/16\right] dx .$$

Mikhail [3, 4] computed $|\delta(t)|^2$ for a flexing missile, neglected the $|\Gamma|^2$ term and assumed that equation (33) was valid for the axial angular momentum for any motion. This assumption is clearly incompatible with equation (31).

The derivative of the angular momentum vector can be computed in the usual way.

$$\frac{d\vec{H}}{dt} = \left(\dot{H}_x, \dot{H}_y, \dot{H}_z\right) + \vec{\Omega} x \vec{H} . \tag{34}$$

For a slender missile $I_t \cong md^2L^2/12$ and $\dot{J}_8$ can be neglected in comparison with $\ddot{J}_6$. The differential equations for the missile's angular motion are

$$I_x \dot{p} + md^2 R\left\{\dot{J}_7 - \dot{Q}\bar{J}_6\right\} = M_x ; \tag{35}$$

$$I_t \dot{Q} - ipI_x Q + imd^2 \ddot{J}_6 = M . \tag{36}$$

Equations (27), (29), and (36) can now be combined to give a simple second order differential equation ξ and various integrals of δ.

$$I_t \ddot{\xi} + \left(a_2 - ipI_x\right)\dot{\xi} + \left(a_1 + ipa_3\right)\xi = J_E + J_N + md^2 \ddot{J}_6 , \tag{37}$$

where

$a_1 = -\left(g_1 d\right)\left[C_{M\alpha} + g_3 C_{L\alpha} C_{Mq}\right]$,

$a_3 = -\left(g_1 d^2/V\right) g_x C_{L\alpha}$,

$a_2 = -\left(g_1 d^2/V\right)\left(C_{Mq} + C_{M\dot{\alpha}} - g_t C_{L\alpha}\right)$,

$g_3 = \rho Sd/2m$,

$g_t = I_t/md^2$, and

J_E, J_N is defined in Appendix B.

For a typical missile g_3 is less than 10^{-4} and the second term in a_1 can be neglected* as well as a similar term in J_N. As a general rule, iQ can replace $\dot{\xi}$ in all the aerodynamic force and aerodynamic moment expressions. The rigid projectile frequencies and damping rates can be computed from equation (37) for

*For lighter than air dirigibles, g_3 is greater than 0.1, and this term makes a statically unstable airship stable in flight [14].

the right hand side set equal to zero. According to Murphy [15], very good approximations for the frequencies are

$$\begin{aligned}\dot{\phi}_{kR} &= \left[pI_x \pm \sqrt{(pI_x)^2 + 4I_t a_1}\right]/2I_t \quad ; \; k = 1, 2, \\ &\cong \pm\omega_R + \left(1 \pm pI_x/4I_t\omega_R\right)pI_x/2I_t\end{aligned} \tag{38}$$

where

$\omega_R = \sqrt{a_1/I_t}$ is the rigid projectile zero-spin frequency.

Exact relations for the damping rates are

$$\lambda_{kR} = -\left(a_2\dot{\phi}_{kR} + pa_3\right)/\left(2\dot{\phi}_{kR}I_t - pI_x\right). \tag{39}$$

The aerodynamic roll moment is the X-component of the aerodynamic moment about the projectile's cm. The linear roll moment coefficient for a rigid finned projectile is usually expressed in terms of a roll-damping coefficient and a steady state spin.

$$\left(C_\ell\right)_{linear} = C_{\ell p}\left(p - p_{ss}\right)\left(d/V\right). \tag{40}$$

The steady-state spin is usually determined by a differential canting of the fins caused either intentionally by the designer or unintentionally by damage to the projectile.

The roll moment of one of the projectile's thin disks is the sum of the linear roll moment it has as part of a projectile and the quadratic roll moment induced by the transverse aerodynamic force acting on its lateral displacement relative to the missile's cm. If we retain only the dominant c_{f1} term in equation (16), the quadratic roll moment has the form:

$$\begin{aligned}\left(dM_x\right)_{quadratic} &= \left[\left(dF_z\right)\delta_y - \left(dF_y\right)\delta_z\right] \\ &= \left(g_1 d\right)c_{f1}R\left\{i\left[\left(\xi - \Gamma\right) + \left(\dot{\delta}_E - ixQ\right)\left(d/V\right)\right]\bar{\delta}\right\}dx .\end{aligned} \tag{41}$$

Therefore, the total aerodynamic roll moment acting on the projectile is

$$M_x = \left(g_1 d\right)\left[\left(C_\ell\right)_{linear} + R\left\{J_9(t)\right\}\right], \tag{42}$$

where J_9 is defined in Appendix B.

The nonlinear roll moment from equation (42) can be placed in the spin equation, equation (35) to yield

$$g_x\dot{p} + R\left\{\dot{J}_7 - \dot{Q}\,\bar{J}_6 - g_2 J_9\right\} = g_2\left(C_\ell\right)_{linear} . \tag{43}$$

This equation is nonlinear due to the retention of all three quadratic terms.

5. Flexing Motion of the Projectile

Classical beam theory for a circular beam assumes the beam to be slender and the elastic moment exerted on the right of a cross-sectional disk, M_e, is proportional to the second derivative of the displacement of the beam. Although this is usually stated in a coordinate system rotating with the beam, the rotational symmetry of the beam allows us to state the proportionality in the non-spinning coordinates.

$$-iM_e = (EI/d)\frac{\partial^2 \delta_E}{\partial x^2}, \tag{44}$$

where

$M_e = M_{ey} + iM_{ez}$,

$Id^{-4} = \iint y^2 dydz = \iint z^2 dydz$ is the area moment of rod, and

E is Young's modulus of elasticity.

A similar proportionality for the elastic shear force exerted on the right can be obtained from beam theory.

$$\hat{F}_e = -\frac{\partial\left((EI/d^2)\frac{\partial^2 \delta_E}{\partial x^2}\right)}{\partial x}. \tag{45}$$

For a homogenous circular rod with constant diameter, EI is constant and the elastic shear force on a disk is

$$\frac{\partial \hat{F}_e}{\partial x}dx = -\rho_1 d^2 \omega_0^2 \frac{\partial^4 \delta_E}{\partial x^4}dx, \tag{46}$$

where

$\omega_0^2 = EI/\rho_1 d^4$.

$\hat{\omega}_0$ has the dimensions of a frequency and appears in the expression for the flexing frequencies of a free-free beam with no aerodynamic force present.

$$\omega_K = (\lambda_K/L)^2 \omega_0, \tag{47}$$

where

$\lambda_K = 4.730, 7.853, 10.996, 14.137\ldots$

A very common beam-damping assumption is the Kelvin-Voight model [15], which requires the beam-damping shear force to be proportional to the time derivative of the elastic shear force. This time derivative, however, must be taken in rod-fixed coordinates that rotate with the rod.

$$\frac{\partial \hat{F}_d}{\partial x} dx = -\rho_1 d^2 \omega_0^2 \hat{k}\, c_{d4} dx\,, \tag{48}$$

where

$$c_{dr} = 2\omega_1^{-1}\left[\frac{\partial}{\partial t}\left(\frac{\partial^r \delta_E}{\partial x^r} e^{-i\phi}\right)\right] e^{i\phi}$$

, and

$$= 2\omega_1^{-1}\frac{\partial^r}{\partial x^r}\left(\dot{\delta}_E - ip\delta_E\right)$$

$\hat{k}$ is a small dimensionless beam-damping coefficient.

c_{dr} is scaled by $2\omega_1^{-1}$ so that $\hat{k} = 1$ corresponds to critical damping of the first elastic mode.

The aerodynamic shear force is a combination of the aerodynamic force distributions $c_{f1}(x), c_{f2}(x)$ given by equation (16) and the drag-induced moment distribution $c_D(x)\delta(x)$ appearing in equation (28). According to reference [16], this aerodynamic shear force is

$$\frac{\partial \hat{F}_a}{\partial x} dx = \left[\frac{\partial F}{\partial x} - g_1 \frac{\partial (c_D \delta)}{\partial x}\right] dx\,. \tag{49}$$

Although c_{f1} and c_{f2} can have a finite number of jump discontinuities, c_D must be continuous and have only a finite number of jump discontinuities in its derivative.

The acceleration of a disk relative to the cm can be obtained by differentiating equation (9). The linear expression for the lateral components of this acceleration is

$$a_{dcy} + i a_{dcz} = \left(\ddot{\delta} - ix\dot{Q}\right) d\,. \tag{50}$$

According to equation (26), the lateral component of the acceleration of the cm is F/m, and the equation of motion for each disk is, therefore,

$$\left(\rho_1 d^2\right)\left(\ddot{\delta} - ix\dot{Q} + F/md\right) = \frac{\partial}{\partial x}\left(\hat{F}_e + \hat{F}_d + \hat{F}_a\right). \tag{51}$$

The aerodynamic force distribution and its integral, $\frac{\partial F}{\partial x}, F$, are available from equations (16) and (22) and the other quantities are provided by equations (46), (48), and (49).

$$\frac{\partial^2 \delta_E}{\partial t^2} + \omega_0^2 \frac{\partial^4 \delta_E}{\partial x^4} + \omega_0^2 \hat{k} c_{d4} - g_2 L\left[c_{f1}\Gamma + \left(c_{f2}\dot{\Gamma} - c_{f1}\dot{\delta}_E\right)(d/V) - \frac{\partial (c_D \delta)}{\partial x}\right] = \tag{52}$$

$$E_1\xi + E_2\dot{\xi} + ix\dot{Q} - N$$

where

$E_j(x)$ is defined in Appendix B.

Equation (52) is based on the usual assumptions of neglecting the canting inertia of the spinning disks and any shear deformation. These small effects can be calculated if desired [17].

The boundary conditions at x_1 are determined by the aerodynamic force and moment exerted on the overhanging fins. The elastic force conditions have an additional term from the drag-induced moment distribution [17].

$$\frac{\partial^3 \delta_E(x_1,t)}{\partial x^3} + \hat{k} c_{d3}(x_1,t) + g_4 c_D(x_1)\delta(x_1,t) = -(g_4/g_1)\int_{x_0}^{x_1} \frac{\partial F}{\partial x} dx = -g_4 f_1; \tag{53}$$

$$\frac{\partial^2 \delta_E(x_1,t)}{\partial x^2} + \hat{k} c_{d2}(x_1,t) = (g_4/g_1)\int_{x_0}^{x_1}\left[(x-x_1)\frac{\partial F}{\partial x} - \delta g_1 c_D\right] dx = g_4 m_1, \tag{54}$$

where

$g_4 = g_2 L/\omega_0^2$, and

f_j, m_j are defined in Appendix B.

Similarly, the boundary conditions at x_2 are set by the aerodynamic force and moment exerted on the nose extension

$$\frac{\partial^3 \delta_E(x_2,t)}{\partial x^3} + \hat{k} c_{d3}(x_2,t) + g_4 c_D(x_2)\delta(x_2,t) = (g_4/g_1)\int_{x_2}^{x_3} \frac{\partial F}{\partial x} dx = g_4 f_2; \tag{55}$$

$$\frac{\partial^2 \delta_E(x_2,t)}{\partial x^2} + \hat{k} c_{d2}(x_2,t) = -(g_4/g_1)\int_{x_2}^{x_3}\left[(x-x_2)\frac{\partial F}{\partial x} - \delta g_1 c_D\right] dx = -g_4 m_2. \tag{56}$$

If beam damping and drag are neglected and the aerodynamic structure does not extend beyond the rod ($\hat{k} = c_D = x_{01} = x_{23} = 0$), the boundary conditions reduce

to those for a free-free beam,

$$\frac{\partial^3 \delta_E}{\partial x^3} = \frac{\partial^2 \delta_E}{\partial x^2} = 0 \quad ; x = x_1, x_2. \tag{57}$$

A fourth-order partial differential equation usually has four boundary conditions. In this case, however, there are two more conditions at x = 0.

$$\delta_E(0) = 0; \tag{58}$$

$$\frac{\partial \delta_E(0)}{\partial x} = 0. \tag{59}$$

These conditions look like the usual cantilever boundary conditions but actually are specified by the motion of the coordinate system which is attached to the missile at the midpoint and tangent to it there. These midpoint conditions can be easily satisfied for a finite element calculation and need not be used as boundary conditions. Calculations of special solutions that assume a single frequency harmonic time variation and involve ordinary differential equations have difficulty satisfying the midpoint conditions. In this report, these solutions will be calculated by pairs of differential equations in x for the aft and fore section of the rod ($x_1 \le x \le 0$; $0 \le x \le x_2$). Equations (53), (54), (58), and (59) are boundary conditions for the aft part and equations (55), (56), (58), and (59) are boundary conditions for the fore part. This use of six boundary conditions implies discontinuities in $\frac{\partial^2 \delta_E}{\partial x^2}, \frac{\partial^3 \delta_E}{\partial x^3}$ at the central junction point. These six boundary conditions for the ordinary differential equations in x are not, however, independent, and it can be shown that equations (53) and (54) imply equations (55) and (56) and vice versa (Appendix C). Thus, the calculations should not show discontinuities in shear force and moment at the junction point.

6. Bent Missile

If the rod were inelastically deformed on launch, its shape would be represented by the sum of a fixed deformation rotating with the missile and an elastic deformation,

$$\delta_E = \tilde{\delta}_E(x,t) + \delta_{EB}(x)e^{i\phi}, \tag{60}$$

where

$$\delta_{EB}(0) = \frac{d\delta_{EB}(0)}{dx} = 0, \text{ and}$$

$p = \dot{\phi}$.

The local inclination of the rod and the lateral location of the cm become

$$\Gamma = \tilde{\Gamma} + \Gamma_B e^{i\phi}; \tag{61}$$

$$\delta_c = \tilde{\delta}_c + \delta_{cB} e^{i\phi}, \tag{62}$$

where

$\tilde{\Gamma} = \dfrac{\partial \tilde{\delta}_E}{\partial x}$,

$\Gamma_B = \dfrac{d\delta_{EB}}{dx}$,

$\tilde{\delta}_c = (1/L)\int_{x_1}^{x_2} \tilde{\delta}_E \, dx$, and

$\delta_{cB} = (1/L)\int_{x_1}^{x_2} \delta_{EB} dx$.

The location of the centerline of the disks relative to the projectile cm is

$$\delta = \tilde{\delta}_E - \tilde{\delta}_c + \delta_B e^{i\phi}, \tag{63}$$

where

$\delta_B = \delta_{EB} - \delta_{cB}$.

For the rigid aerodynamic structure extension,

$$\begin{aligned} \delta_{EB}(x) &= \delta_{EB}(x_1) + (x - x_1)\Gamma_B(x_1); \qquad x_0 \le x \le x_1; \\ \delta_{EB}(x) &= \delta_{EB}(x_2) + (x - x_2)\Gamma_B(x_2); \qquad x_2 \le x \le x_3. \end{aligned} \tag{64}$$

Now Γ_B produces an aerodynamic force and moment that rotates with the projectile. If the fins are bent with respect to the rod, an additional differential force that rotates with the missile is produced and must be added to equation (16).

$$dF_{BF} = g_1 c_{f1} \Gamma_{BF}(x) e^{i\phi} dx, \tag{65}$$

where

$\Gamma_{BF}(x)$ is a measure of bent fin damage.

The aerodynamic force acting on the bent missile is

$$F = -g_1 \left\lfloor C_{N\alpha}\xi + (C_{N\dot{\alpha}} + C_{Nq})(\dot{\xi} d/V) - J_1(t) - \dot{J}_2(t)(d/V) - C_{NBF} e^{i\phi} \right\rfloor, \tag{66}$$

where C_{NBF} is defined in Appendix A.

If the fin damage extends beyond the rear end of the rod, it will exert an additional force and moment on the rod at $x = x_1$. This bent fin force term also has to be included in the quadratic roll moment appearing in equation (43).

$$g_x\dot{p} + R\left\{\dot{J}_7 - \dot{Q}\bar{J}_6 - g_2\left(J_9 + J_{9BF}\right)\right\} = g_2\left(C_\ell\right)_{linear}, \tag{67}$$

where

$$J_{9BF} = -ie^{i\phi}\int_{x_0}^{0} c_{f1}\Gamma_{BF}\bar{\delta}dx.$$

Equation (27) for the cm of the elastic missile becomes

$$(V/d)\left(\dot{\xi} - iQ\right) = -g_2\left(C_{L\alpha}\xi - C_{NBF}e^{i\phi}\right) + N. \tag{68}$$

The aerodynamic moment as given by equation (29) becomes

$$M = -i(g_1 d)\left[C_{M\alpha}\xi + \left(C_{M\dot{\alpha}} + C_{Mq}\right)\left(\dot{\xi}d/V\right) - J_3(t) - \dot{J}_4(t)(d/V) - J_5(t) - C_{MBF}e^{i\phi}\right], \tag{69}$$

where

C_{MBF} is defined in Appendix A.

The projectile angular motion equation (36) becomes

$$I_t\dot{Q} - ipI_x Q = -i(g_1 d)\left[C_{M\alpha}\xi + \left(C_{M\dot{\alpha}} + C_{Mq}\right)\left(\dot{\xi}\,d/V\right) - C_{MBF}e^{i\phi}\right] - iJ_E - imd^2J_6. \tag{70}$$

In the flexing motion equation (51), δ_E is replaced by $\tilde{\delta}_E$ in the elastic and damping force terms, and the bent fin terms are added to F and F_a to obtain the partial differential equation for a bent missile.

$$\frac{\partial^2\tilde{\delta}_E}{\partial t^2} + \omega_0^2\frac{\partial^4\tilde{\delta}_E}{\partial x^4} + \omega_0^2\hat{k}\tilde{c}_{d4} - g_2L\left[c_{f1}\Gamma + \frac{\partial}{\partial t}\left(c_{f2}\Gamma - c_{f1}\delta_E\right)(d/V) - \frac{\partial(c_D\delta)}{\partial x}\right] \tag{71}$$
$$= E_1\xi + E_2\dot{\xi} + ix\dot{Q} - N - E_{BF}e^{i\phi}.$$

In the boundary conditions specified by equations (53)-(56), δ_E is replaced by $\tilde{\delta}_E$ in the partial derivatives on the left side of the equations. The conditions at x_1 are modified by force or moment contributions from any fin damage between x_0 and x_1 that may have occurred.

7. Trim Solution

The general solution for the motion of a bent missile requires the numerical integration of one partial differential equation (equation [71]) and three ordinary

differential equations (equations [67-69]). A simple special solution is that for the steady state motion of a bent missile with a constant spin. This motion is called trim motion and has the form

$$\xi = \xi_T e^{ipt}; \tag{72}$$

$$\tilde{\delta}_E = \tilde{\delta}_{ET} e^{ipt}; \tag{73}$$

$$\tilde{\Gamma} = \tilde{\Gamma}_T e^{ipt}; \tag{74}$$

$$\delta_E = \left(\delta_{EB} + \tilde{\delta}_{ET}\right) e^{ipt} = \delta_{ET} e^{ipt}; \tag{75}$$

$$\Gamma = \left(\Gamma_B + \tilde{\Gamma}_T\right) e^{ipt} = \Gamma_T e^{ipt}. \tag{76}$$

For this motion, beam damping is zero ($\tilde{c}_{dr} = 0$).

Equation (68) can now be used to eliminate Q and $\dot{Q}$ from equations (70) and (71) and equations (72–76) inserted to yield:

$$b_1 \xi_T = J_{ET} + J_{NT} + J_{BF} - md^2 p^2 J_{6T}; \tag{77}$$

$$\frac{d^4 \tilde{\delta}_{ET}}{dx^4} - E_4 \frac{d\tilde{\delta}_{ET}}{dx} + E_5 \tilde{\delta}_{ET} - g_4 \tilde{\delta}_{Tc} \frac{dc_D}{dx} = E_3 \xi_T - N_T^* - E_{BF}^* + E_B, \tag{78}$$

where $J_{ET}, J_{NT}, J_{BF}, b_1, E_j, E_B, N_T^*, E_{BF}^*$ are defined in Appendix D.

Boundary conditions as given by modified equations (53)-(56), (58), and (59) become

$$\frac{d^3 \tilde{\delta}_{ET}(x_1)}{dx^3} + g_4 c_D(x_1) \delta_T(x_1) = -g_4 f_{1T}; \tag{79}$$

$$\frac{d^2 \tilde{\delta}_{ET}(x_1)}{dx^2} = g_4 m_{1T}; \tag{80}$$

$$\frac{d^3 \tilde{\delta}_{ET}(x_2)}{dx^3} + g_4 c_D(x_2) \delta_T(x_2) = g_4 f_{2T}; \tag{81}$$

$$\frac{d^2 \tilde{\delta}_{ET}(x_2)}{dx^2} = -g_4 m_{2T}; \tag{82}$$

$$\tilde{\delta}_{ET}(0) = 0; \tag{83}$$

$$\frac{d\tilde{\delta}_{ET}(0)}{dx} = 0, \tag{84}$$

where f_{jT}, m_{jT} are defined in Appendix D.

These boundary conditions can be satisfied by expressing $\tilde{\delta}_{ET}$ as the sum of three functions of x,

$$\tilde{\delta}_{ET}(x) = w_1(x) + B_2 w_2(x) + B_3 w_3(x). \tag{85}$$

The first function is the solution of the following differential equation and initial conditions

$$\frac{d^4 w_1}{dx^4} - E_4 \frac{dw_1}{dx} + E_5 w_1 = E_3 \xi_T - N_T^* - E_{BF}^* + E_B + g_4 \tilde{\delta}_{cT} \frac{dc_D}{dx}, \tag{86}$$

where

$$w_1(0) = \frac{dw_1(0)}{dx} = \frac{d^2 w_1(0)}{dx^2} = \frac{d^3 w_1(0)}{dx^3} = 0.$$

The other two functions are solutions of the homogenous equation with different initial conditions.

$$\frac{d^4 w_m}{dx^4} - E_4 \frac{dw_m}{dx} + E_5 w_m = 0; \qquad m = 2, 3, \tag{87}$$

where

$$w_2(0) = \frac{dw_2(0)}{dx} = \frac{d^2 w_2(0)}{dx^2} = 0,$$

$$w_3(0) = \frac{dw_3(0)}{dx} = \frac{d^3 w_3(0)}{dx^3} = 0, \text{ and}$$

$$\frac{d^3 w_2(0)}{dx^3} = \frac{d^2 w_3(0)}{dx^2} = 1.$$

Equations (86) and (87) can be integrated from zero toward negative x or toward positive x. $w_{m1}(x)$ denotes w_m for negative x, and $w_{m2}(x)$ denotes w_m for positive x. B_{21}, B_{31} are values of B_2, B_3 which satisfy equations (79) and (80), and B_{22}, B_{32} are those values which satisfy equations (81) and (82). The values should be close to each other and their difference is a measure of the accuracy of various approximations and the numerical integration process.

The presence of the constants $N_T, \xi_T, \tilde{\delta}_c$ in equations (77) and (86) and the boundary conditions present some difficulty because they involve integrals of $\tilde{\delta}_{ET}$ and its first derivative. Our numerical technique is to replace these constants with guessed values $N_{T0}, \xi_{T0}, \tilde{\delta}_{c0}$ and use an iterative three-dimensional Newton's Method to converge on the proper values. The partial derivatives used in Newton's Method are computed by the Chapman-Kirk [18]

technique. If drag is neglected, the need to know $\tilde{\delta}_c$ vanishes, and this reduces to a two-dimensional process. This process, of course, depends on reasonably good first guesses.

For trim motion $\dot{p} = \dot{J}_7 = 0, \ddot{Q} = ip^2\xi_T$ and equation (67) become a simple equality of two functions of p.

$$f_2(p) = f_1(p), \tag{88}$$

where

$f_1 = p - p_{ss}$,

$f_2 = -R\{i(p^2/g_2)\xi_T\bar{J}_{6T} + J_{9T}\}(C_{\ell p}d/V)^{-1}$, and

$$J_{9T} = i\int_{x_0}^{x_3} c_{f1}[(\xi_T - \Gamma_T - \Gamma_{BF}) + i(\delta_{ET} - x\xi_T)(pd/V)]\bar{\delta}_T dx.$$

Equilibrium values of spin are determined by the intersection of these two curves. The stability of an equilibrium spin can be found by the integration of equations (67), (68), (70), and (71), for nonconstant spin near an equilibrium spin. The stable equilibrium spins locate spin lock-in possibilities.

8. Transient Solutions

A rigid symmetric-finned missile flying with constant spin has two natural frequencies, $\dot{\phi}_{1R}$ and $\dot{\phi}_{2R}$, where $\dot{\phi}_{1R} \cong -\dot{\phi}_{2R}$. Each of the flexing frequencies given by equation (47) would give rise to two coning frequencies, $\pm\omega_K$. The frequencies present in the motion of an elastic projectile would form an infinite sequence where the first two would be related to $\dot{\phi}_{1R}$ and $\dot{\phi}_{2R}$, whereas the later ones would evolve from $\pm\omega_K$, i.e., $(\dot{\phi}_{2K+1} \cong \omega_K \; ; \dot{\phi}_{2K+2} \cong -\omega_K)$. The odd numbered modes have positive frequencies and are called positive modes, whereas the even numbered modes are called negative modes.

Transient solutions of equations (70) and (71) are solutions of the homogeneous form of these equations. $(\delta_B = \Gamma_B = C_{NBF} = C_{MBF} = 0)$. Special transient solutions of equations (70) and (71) have the form

$$\xi = T_k e^{A_k t}; \tag{89}$$

$$\delta_E = \psi_k(x)T_k e^{A_k t}. \tag{90}$$

where,

$A_k = \lambda_k + i\dot{\phi}_k$

$T_k = K_{k0} e^{i\phi_{k0}}$.

Equation (68) can be used again to eliminate Q and $\dot{Q}$ from equations (70), (71), (89), and (90) inserted to yield

$$b_{1k} = J_{Ek} + J_{Nk} + md^2 A_k^2 J_{6k}; \tag{91}$$

$$E_{6k}\frac{d^4\psi_k}{dx^4} - E_{4k}\frac{d\psi_k}{dx} + E_{5k}\psi_k - g_4\psi_{kc}\frac{dc_D}{dx} = E_{3k} - N_k^*, \tag{92}$$

where $b_{jk}, J_{Ek}, J_{Nk}, E_{jk}, \psi_{kc}, N_K^*$ are defined in Appendix E.

These equations and their boundary conditions can be solved in a manner quite similar to that used for the trim solution by the introduction of three auxiliary functions.

$$\psi_k(x) = w_4(x) + B_5 w_5(x) + B_6 w_6(x). \tag{93}$$

w_4 is the solution of the following differential equation and initial conditions:

$$E_{6k}\frac{d^4 w_4}{dx^4} - E_{4k}\frac{dw_4}{dx} + E_{5k} w_4 = -E_{3k} - N_k^* + g_4\psi_{kc}\frac{dc_D}{dx}, \tag{94}$$

where

$$w_4(0) = \frac{dw_4(0)}{dx} = \frac{d^2 w_4(0)}{dx^2} = \frac{d^3 w_4(0)}{dx^3} = 0.$$

The other two functions satisfy the homogeneous equation with different initial conditions

$$E_{6k}\frac{d^4 w_m}{dx^4} - E_{4k}\frac{dw_m}{dx} + E_{5k} w_m = 0;\ m = 5, 6, \tag{95}$$

where

$$w_5(0) = \frac{dw_5(0)}{dx} = \frac{d^2 w_5(0)}{dx^2} = 0,$$

$$w_6(0) = \frac{dw_6(0)}{dx} = \frac{d^3 w_6(0)}{dx^3} = 0, \text{ and}$$

$$\frac{d^3 w_5(0)}{dx^3} = \frac{d^2 w_6(0)}{dx^2} = 1.$$

The parameters B_{51}, B_{61} are values of B_5, B_6 that satisfy the boundary conditions at x_1:

$$\frac{d^3\psi_k}{dx^3} + g_4 E_{6k}^{-1} c_D (\psi_k - \psi_{kc}) = -g_4 E_{6k}^{-1} f_{1k}; \tag{96}$$

$$\frac{d^2\psi_k}{dx^2} = g_4 E_{6k}^{-1} m_{1k}. \tag{97}$$

Similarly, B_{52}, B_{62} perform the same function at x_2.

$$\frac{d^3\psi_k}{dx^3} + g_4 E_{6k}^{-1} c_D (\psi_k - \psi_{kc}) = g_4 E_{6k}^{-1} f_{2k}; \tag{98}$$

$$\frac{d^2\psi_k}{dx^2} = -g_4 E_{6k}^{-1} m_{2k}. \tag{99}$$

The presence of the parameters N_k^*, A_k, ψ_{kc} complicates these differential equations. N_k^* involves A_k and N_k. The definition of N_k involves integrals of ψ_k and its first derivative and A_k must satisfy equation (91) that contains N_k and integrals ψ_k and its first derivative. Guessed values of these parameters $N_{k0}, A_{k0}, \psi_{kc0}$ are used in equations (94)-(99) and another three-dimensional Newton's Method is used as well. For frequencies greater than $3\omega_R$, a good estimate for z_{c0} is $-N_0 A_{k0}^{-1}$.

9. Flight Motion

The complete flight motion of an elastic bent symmetric projectile with constant spin is described by the sum of a trim mode and an infinity of transient modes. If we limit ourselves to the aerodynamic modes and the first two elastic modes, the pitching motion and the lateral motion of the forward end of the rod can be expressed by two sums of five terms.

$$\xi = \xi_T e^{ipt} + T_1 e^{A_1 t} + T_2 e^{A_2 t} + T_3 e^{A_3 t} + T_4 e^{A_4 t}; \tag{100}$$

$$\delta_E(x_2, t) = \delta_{ET}(x_2) e^{ipt} + \hat{T}_1 e^{A_1 t} + \hat{T}_2 e^{A_2 t} + \hat{T}_3 e^{A_3 t} + \hat{T}_4 e^{A_4 t}, \tag{101}$$

where

$$\hat{T}_k = \psi_k(x_2) T_k = \psi_{k2} T_k.$$

Because ψ_{12} and ψ_{22} are usually less than 0.5 and the angular motion is usually less than 0.1 radian, the motion described by the aerodynamic modes is primarily a pitching motion and is best characterized by (K_1, K_2). $|\psi_{32}|$ and $|\psi_{42}|$ are,

however, usually greater than fifty and the motion described by these flexing modes is primarily a flexing motion. For this reason we will characterize this flexing motion by the modal amplitudes of the rod lateral motion $\left(\hat{K}_{30}, \hat{K}_{40}\right)$.

For a nonspinning missile, equations (91) and (92) imply an important pairing of solutions. If A_k, ψ_k is a solution, $\overline{A}_k, \overline{\psi}_k$ is a solution.

$$\begin{aligned} A_2 &= \overline{A}_1 \qquad \psi_2 = \overline{\psi}_1 \\ A_4 &= \overline{A}_3 \qquad \psi_4 = \overline{\psi}_3 \,. \end{aligned} \tag{102}$$

Thus for zero spin, the negative modes have the same damping as the positive modes, and their waveforms are conjugates of the positive waveforms. For small spin, the magnitudes of the waveforms are essentially equal,

$$|\psi_{12}| \cong |\psi_{22}|; |\psi_{32}| \cong |\psi_{42}| \,. \tag{103}$$

The transient angular motion and the rod lateral motion are both expressed by the sum of two damped elliptical motions with frequencies, $\dot{\phi}_1, \dot{\phi}_3$. The initial semi-major axes of the angular modes are $K_{10} + K_{20}$ and $\left(\hat{K}_{30} + \hat{K}_{40}\right)|\psi_{32}|^{-1}$, whereas the initial semi-minor axes of the angular modes are $|K_{10} - K_{20}|$ and $\left|\hat{K}_{30} - \hat{K}_{40}\right||\psi_{32}|^{-1}$. Similarly, the initial semi-major axes of the rod lateral modes are $(K_{10} + K_{20})|\psi_{12}|$ and $\left(\hat{K}_{30} + \hat{K}_{40}\right)$, whereas the initial semi-minor axes are $|K_{10} - K_{20}||\psi_{12}|$ and $\left|\hat{K}_{30} - \hat{K}_{40}\right|$.

If either motion goes through zero, the elliptical motion would be planar. For gun launch, both the angular and the flexing motion are forced to be near zero initially, and "near planar motion" is expected after launch. Guidos et al. [19] have analyzed the flight motion of long elastic finned projectiles in the U.S. Army Research Laboratory (ARL) Transonic Experimental Facility's non-rotating coordinates and have observed near planar nose-tip motion with an amplitude in excess of 0.5 diameter.

10. Induced Drag

The aerodynamic drag force is directed along the velocity vector and the linear normal force on a disk is perpendicular to the disk axis, which is canted at an angle of $\xi - \Gamma$ with respect to the velocity vector. Thus, the normal force has a quadratic contribution to the drag. This contribution is called induced drag and can be computed for a pitching and flexing missile as

$$g_1 C_{DI} = \int_{x_0}^{x_3} \left[(\beta - \Gamma_y) \frac{\partial F_y}{\partial x} + (\alpha - \Gamma_z) \frac{\partial F_z}{\partial x} \right] dx . \tag{104}$$

Although the nonlinear axial flow along the rod has a quadratic contribution to drag, this contribution is usually significantly less than the induced drag.

The normal force distribution will be approximated by its dominant term, $c_{f1}(\xi - \Gamma)$.

$$\begin{aligned} C_{DI} &= \int_{x_0}^{x_3} c_{f1} (\xi - \Gamma)(\bar{\xi} - \bar{\Gamma}) dx \\ &= C_{N\alpha} |\xi|^2 - \bar{\xi} J_1 - \xi \bar{J}_1 + J_D , \end{aligned} \tag{105}$$

where

$$J_D = \int_{x_0}^{x_3} c_{f1} \Gamma \bar{\Gamma} dx .$$

The first term in equation (105) is the well-known expression for the induced drag of a rigid missile. The induced drag for a particular angular mode is

$$C_{DI\,k} = C_k K_{k0}^2 , \tag{106}$$

where

$C_k = C_{N\alpha} - J_{1k} - \bar{J}_{1k} + J_{Dk}$, and

$$J_{Dk} = \int_{x_0}^{x_3} c_{f1} \frac{d\psi_k}{dx} \frac{d\bar{\psi}_k}{dx} dx .$$

The average induced drag for a missile whose motion contains all five modes of equations (100) and (101) can be computed from the sum of the pure-mode induced drag contributions and the trim induced drag.

$$C_{DI} = C_1 \left(K_{10}^2 + K_{20}^2 \right) + \hat{C}_3 \left(\hat{K}_{30}^2 + \hat{K}_{40}^2 \right) + C_{DIT} , \tag{107}$$

where

$\hat{C}_3 = C_3 |\psi_{33}|^{-2}$, and

$$C_{DIT} = \int_{x_0}^{x_3} c_{f1} \left| \xi_T - \Gamma_T \right|^2 dx .$$

11. Numerical Results

In references [6] and [7], numerical results were obtained for two specific missiles. The first was a flare-stabilized 25-cal. rod flying at 18,000 ft/s considered by Platus [1] and the second was a fin-stabilized 20-cal. rod flying at 6000 ft/s. The flare on the Platus missile was 7.5-cal. long and the flare base diameter was 4 cal., i.e., 4 rod diameters. The finned missile has a 1-cal. nose extension and a 1-cal. fin extension (Figure 1). The necessary parameters for these missiles are given in Appendix F and converged values of A_k, N_k, ψ_{k0} for the finned missile are given in Table 1. The slender missile values of the moments of inertia are given in parenthesis are used in the numerical calculation of the transverse motion. The actual value of I_x should be used in an integration of the roll equation (67).

A measure of the flight flexibility of a missile is the ratio of the first elastic frequency to the rigid missile aerodynamic frequency, $\sigma = \omega_1/\omega_R$. The equations for the transient solution derived in section 8 have been solved for the first aerodynamic frequency, $\dot{\phi}_1$, and the results plotted versus σ for both missiles. In Figure 2, it is shown that this frequency for the flare-stabilized missile is 98% of the rigid missile value for $\sigma = 10$ and decreases as σ decreases. We see that the theory of this report falls between the 3-body theory and the Platus theory.

The remainder of the numerical results was obtained for the finned missile. In Figure 3, this report's theory is compared with the 3-body theory, and we see that it has a similar variation but predicts lower frequencies. Note that the frequency for $\sigma = 5$ is near 60% the rigid missile value. The first two positive flexing frequencies $\dot{\phi}_3/\omega_1, \dot{\phi}_5/\omega_2$ are plotted versus σ in Figure 4. For small σ both frequencies are slightly larger than the free-free beam values, but they approach these values as σ grows.

The magnitude of the forward end motion is plotted against σ in Figure 5. At $\sigma = 5$, we see that 0.1 radian of the positive aerodynamic mode causes 0.18 diameter of flexing motion. For the flexing frequencies, one diameter of flexing motion is associated with 0.018 radian (1.0°) of angular motion for the first positive mode and 0.072 radian (4.1°) of angular motion for the second positive mode.

The forward end of the rod bends away from the velocity vector for an aerodynamic mode $(\psi_{12} \le 0)$ while it bends toward the velocity vector for both the first positive symmetric mode and the first positive antisymmetric mode. The flexing shape of the entire rod is very close to planar for each mode. Thus

$R\{\psi_k(x)/\psi_{k2}\}$ describes the shape of the rod during a modal motion and is plotted versus x for k = 1, 3, 5 in Figure 6. For the first two positive frequencies, the shape is quite similar and the rear end of the rod is deflected about 15% less than the forward end. The third positive mode is antisymmetric and rear end deflects about 5% more than the front end and in the opposite direction.

The damping rates of the three modes for no beam damping $(\hat{k}=0)$ are plotted versus σ in Figure 7. For $\sigma=5$, the first aerodynamic damping rate is 85% of the rigid body damping rate, while the rates for the second and third positive mode damping rate are 75% and 35%, respectively. In Figure 8 λ_1/ω_R is plotted versus p/ω_R for two non-zero values of beam damping and $\sigma=5$. $\dot{\phi}_1/\omega_R$ for this value of σ is 0.6 and beam damping reduces the damping rate when p/ω_R exceeds this value. The behavior was first observed Platus [1] and predicted by the 3-body theory [6, 7].

The induced drag coefficient for the aerodynamic mode, C_1/C_{N_α}, is plotted versus σ in Figure 9. It is 12% less than that for a rigid middle at $\sigma=5$. Although the nose of the elastic missile bends to a larger angle of attack, the fins bend to a lesser angle of attack and the net effect is less induced drag. The induced drag coefficients for the two flexing modes are plotted versus σ in Figure 10. Here we see that for the same amplitude motion the induced drag for the symmetric mode is more than 50% greater than that for the antisymmetric mode. Because both ends of the missile bend to a lesser angle of attack for the antisymmetric mode, this mode should have much smaller induced drag.

For the bent missile calculations we will assume no fin damage $(\Gamma_{BF}=0)$ and the bent rod will be described by a pair of quartic curves.

$$\begin{aligned}\delta_{EB} &= d_{11}x^2 + d_{21}x^4 \qquad -10 \le x \le 0 \\ &= d_{12}x^2 + d_{22}x^4 \qquad 0 \le x \le 10\end{aligned} \tag{108}$$

Equation (62) provides a relation for δ_{cB}.

$$\delta_{cB} = (d_{11}+d_{12})(L/2)^2/6 + (d_{21}+d_{22})(L/2)^4/10. \tag{109}$$

We will assume the rear of the rod is undeformed $d_{11}=d_{12}=0$ and the values of d_{12}, d_{22} are given in Appendix F.

In Figure 11, the magnitude of the ratio of the trim angle of attack to the zero spin trim angle of a rigid missile is plotted versus spin for $\sigma=5$. The zero spin trim angle of the elastic missile is about four times that of a rigid missile. The first resonant peak is near $p/\omega_R=0.6$ and shows a five-fold magnification of the zero spin elastic trim. A smaller resonant peak occurs at the elastic frequency near 5 and much larger resonant peak near 14. The magnitude of the rod

deflection is plotted versus p/ω_R in Figure 12. The trim deflection for the first elastic mode is about eight times that for the aerodynamic mode while the trim deflection for the second elastic mode is three times that for the first elastic mode.

In Figure 13, f_2 is plotted versus p/ω_R. A sample f_1 line for $p_{ss}/\omega_R = 6.5$ is also shown. The intersections of these curves are loci of possible spin-yaw lock-ins. The actual occurrence of lock-in would be shown by integration of the partial differential equation for flexing motion.

12. Summary

1. A system of equations has been derived for the motion of a symmetric elastic missile. This system consists of three ordinary differential equations and one fourth-order partial differential equation. Each of these equations contains integrals of the elastic deformation of the missile.
2. A fourth-order ordinary equation with boundary conditions has been obtained to determine natural frequencies and damping rates of the motion.
3. A simple special ordinary differential equation for the trim motion of a bent missile has been obtained.
4. Equations for nonlinear roll moments for a bent missile have been obtained and a condition for possible spins-yaw lock-in stated.
5. Numerical results have been obtained for the natural frequencies, flexing waveforms, damping rates, and induced drag coefficients.

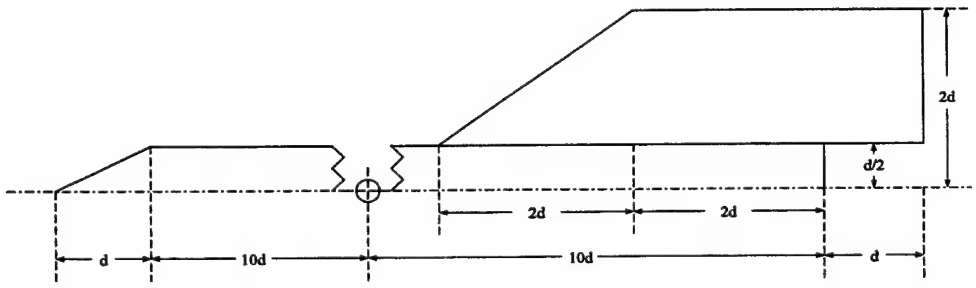

Figure 1. Sketch of finned missile.

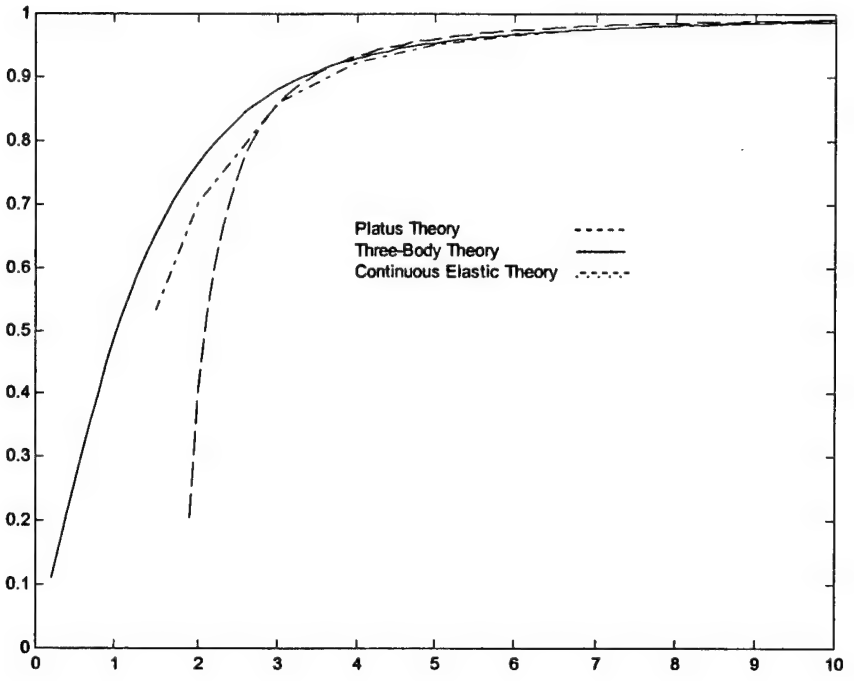

Figure 2. $\dot{\phi}_1/\omega_R$ vs. σ for flare-stabilized rod.

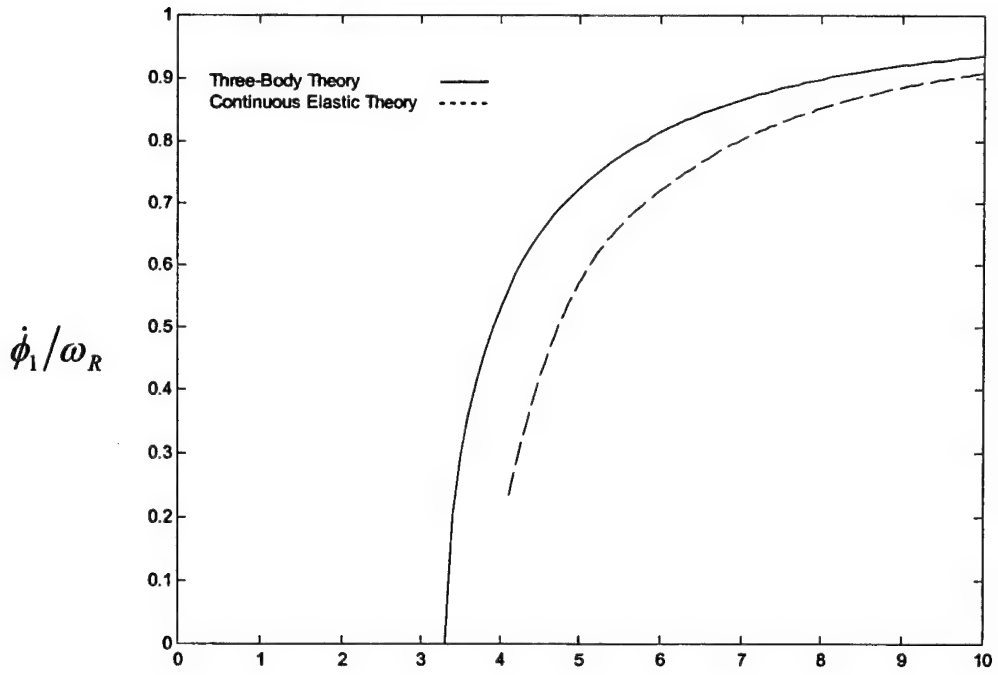

Figure 3. $\dot{\phi}_1/\omega_R$ vs. σ for finned missile.

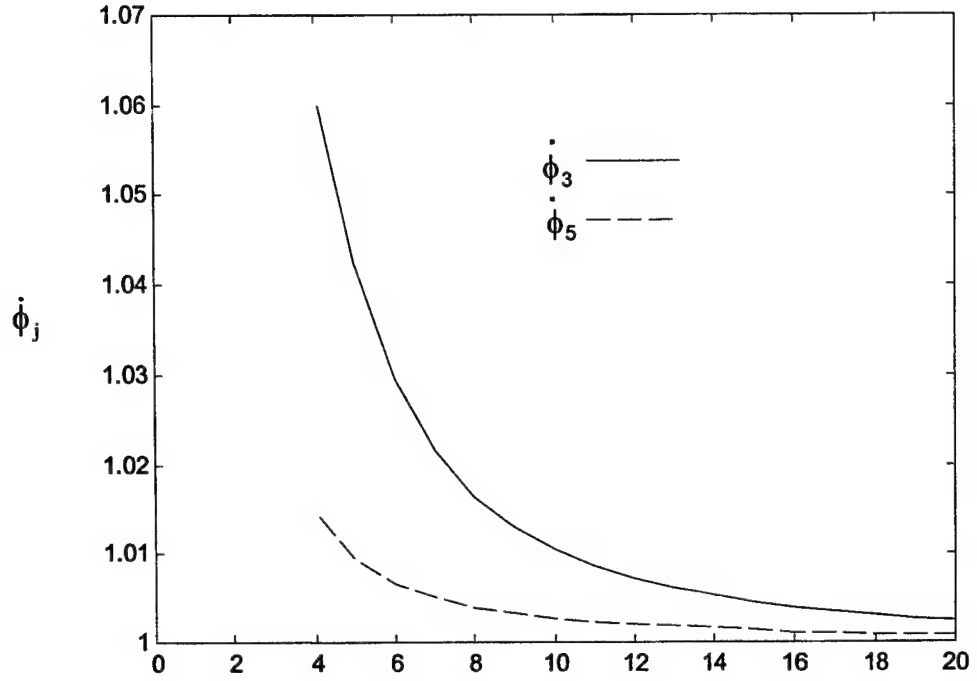

Figure 4. $\dot{\phi}_3/\omega_1, \dot{\phi}_5/\omega_2$ vs. σ for finned missile.

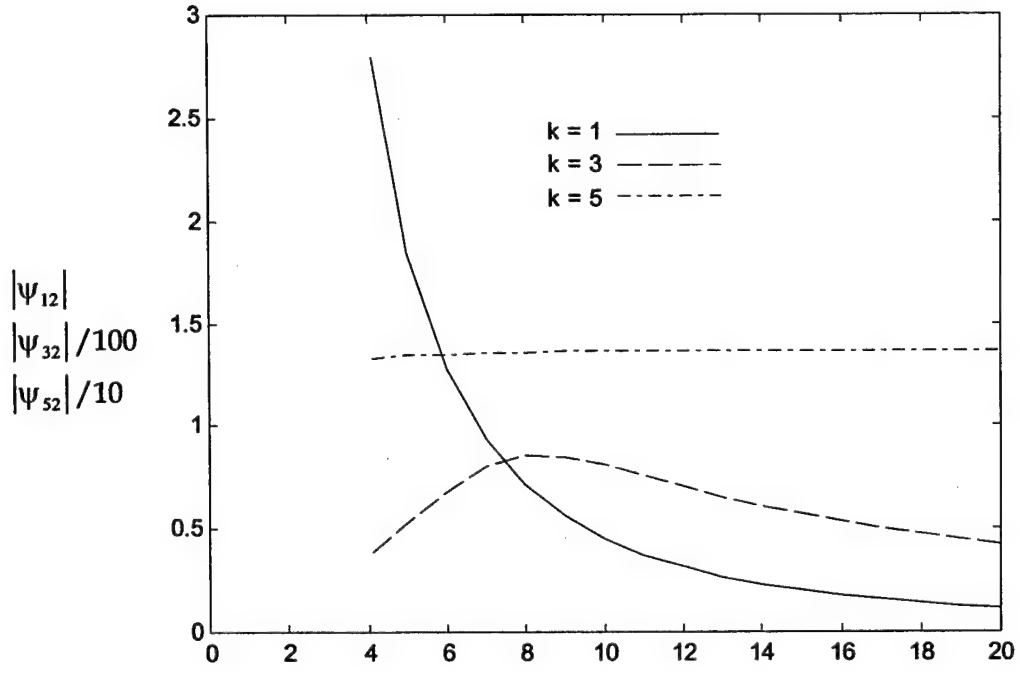

Figure 5. $|\psi_{k2}|$ vs. σ for k = 1, 3, 5.

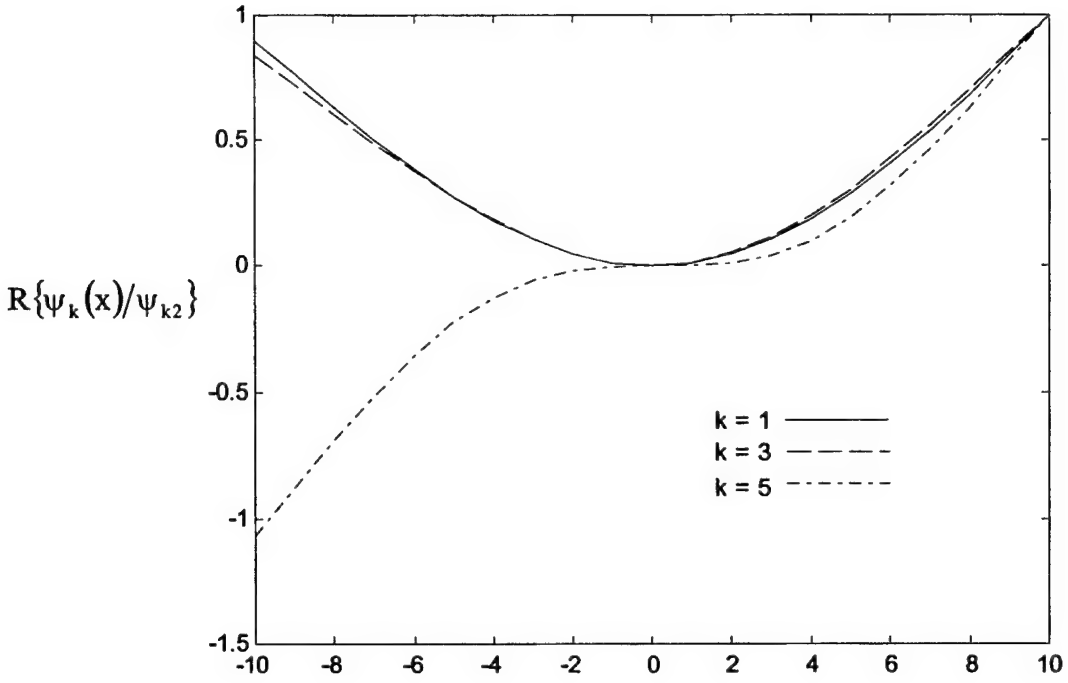

Figure 6. $R\{\psi_k(x)/\psi_{k2}\}$ vs. x for $\sigma = 5$, k = 1, 3, 5.

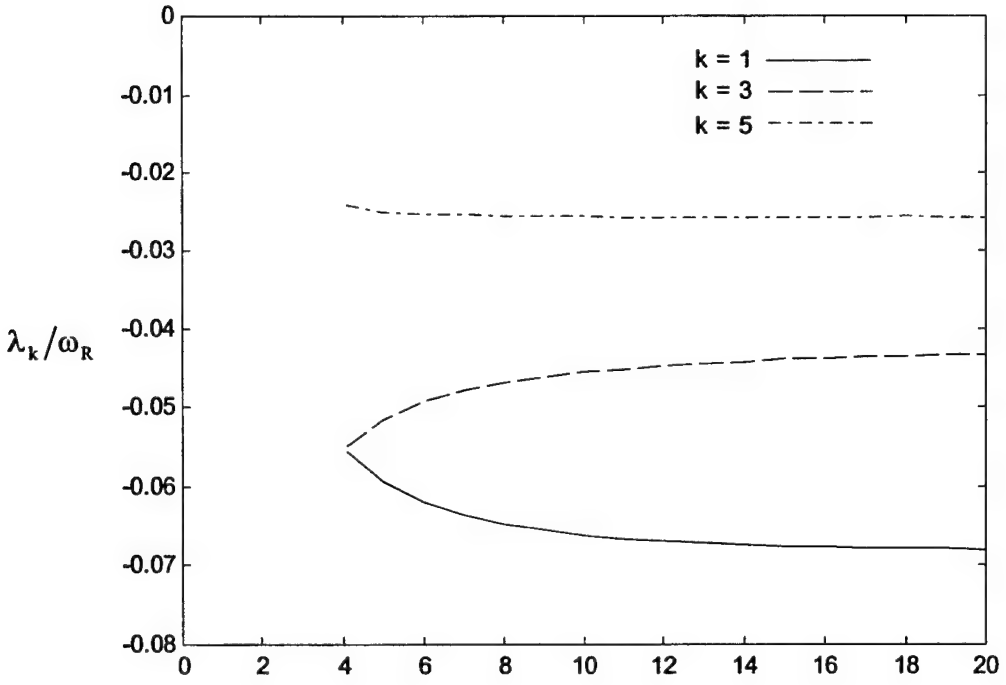

Figure 7. λ_k/ω_R vs. σ for k = 1, 3, 5.

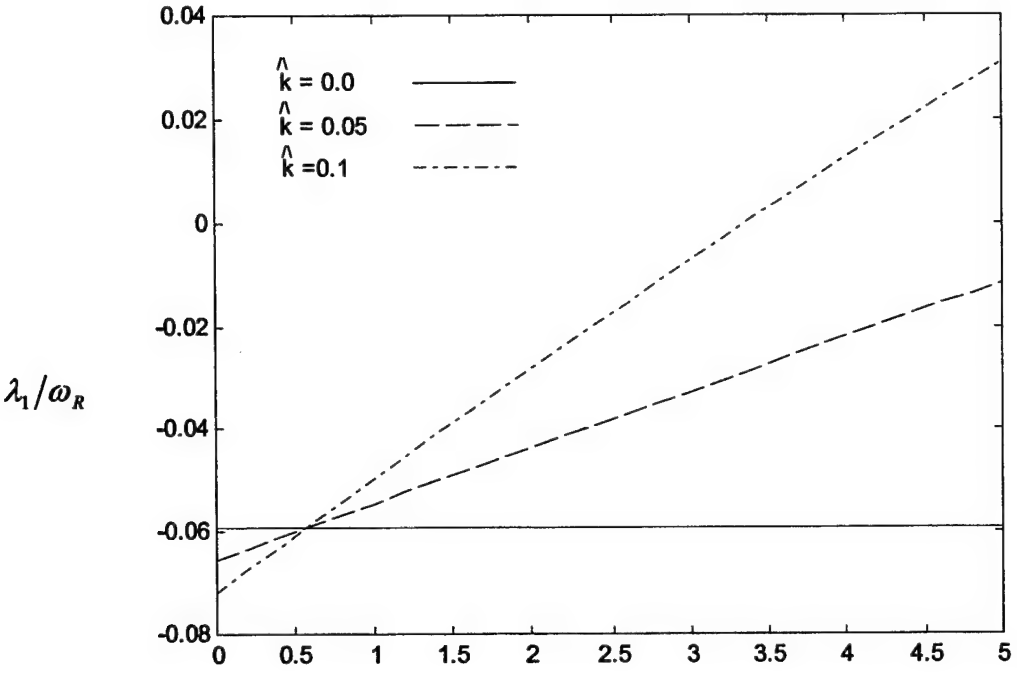

Figure 8. λ_1/ω_R vs. p/ω_R for $\sigma = 5, \hat{k} = 0, 0.05, 0.10$.

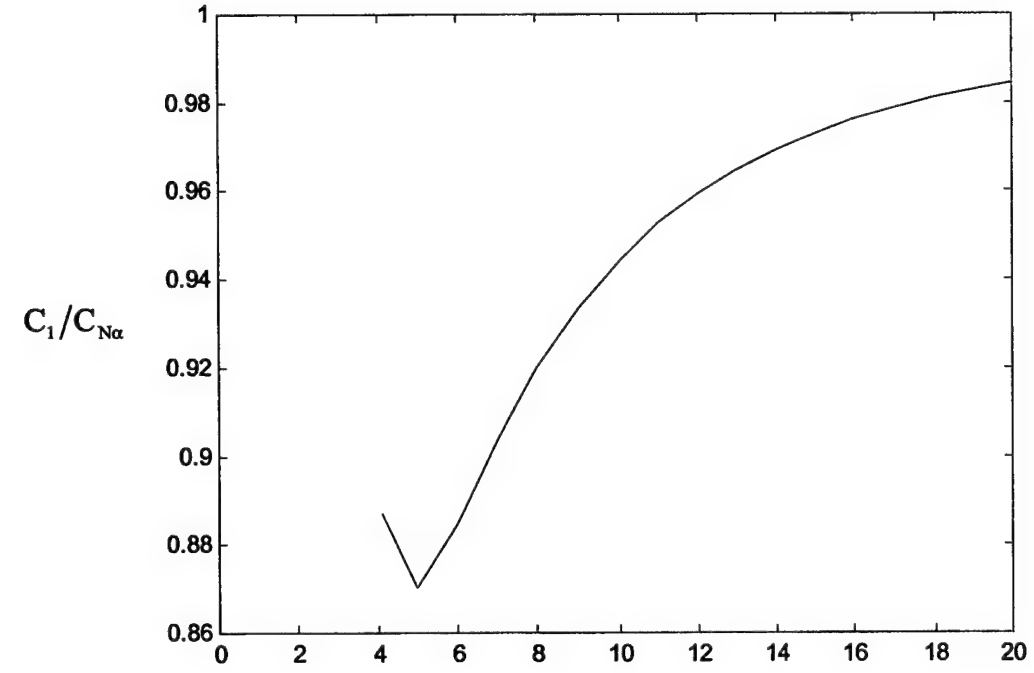

Figure 9. $C_1/C_{N\alpha}$ vs. σ.

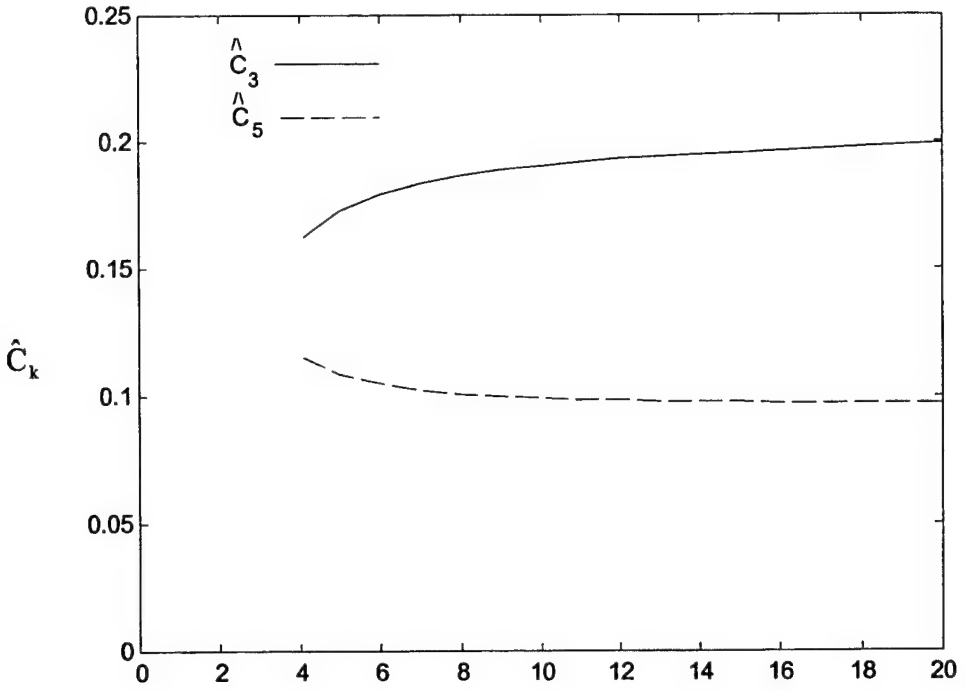

Figure 10. $\hat{C}_k$ vs. σ for k = 3, 5.

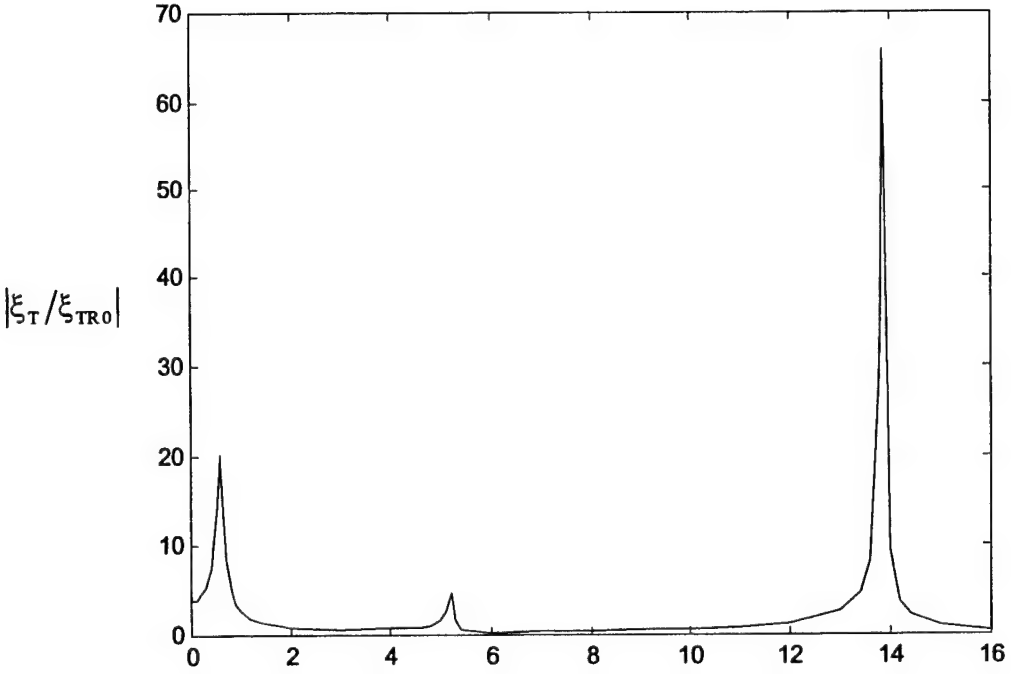

Figure 11. $|\xi_T/\xi_{TR0}|$ vs. p/ω_R for bent-finned missile at $\sigma = 5$.

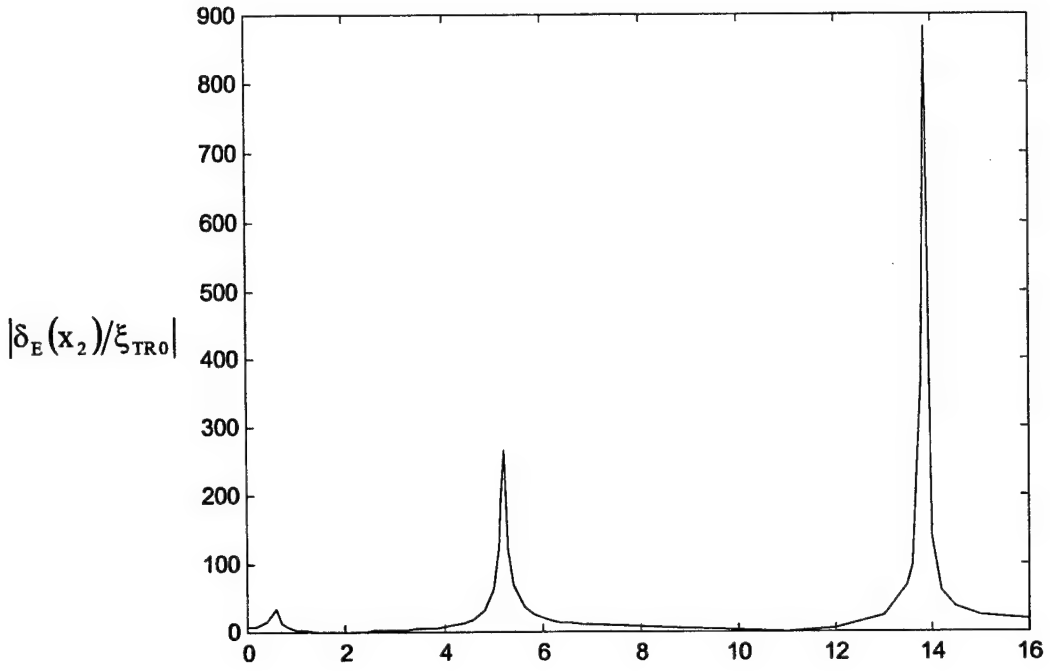

Figure 12. $|\delta_E(x_2)/\xi_{TR0}|$ vs. p/ω_R at $\sigma = 5$ for bent-finned missile.

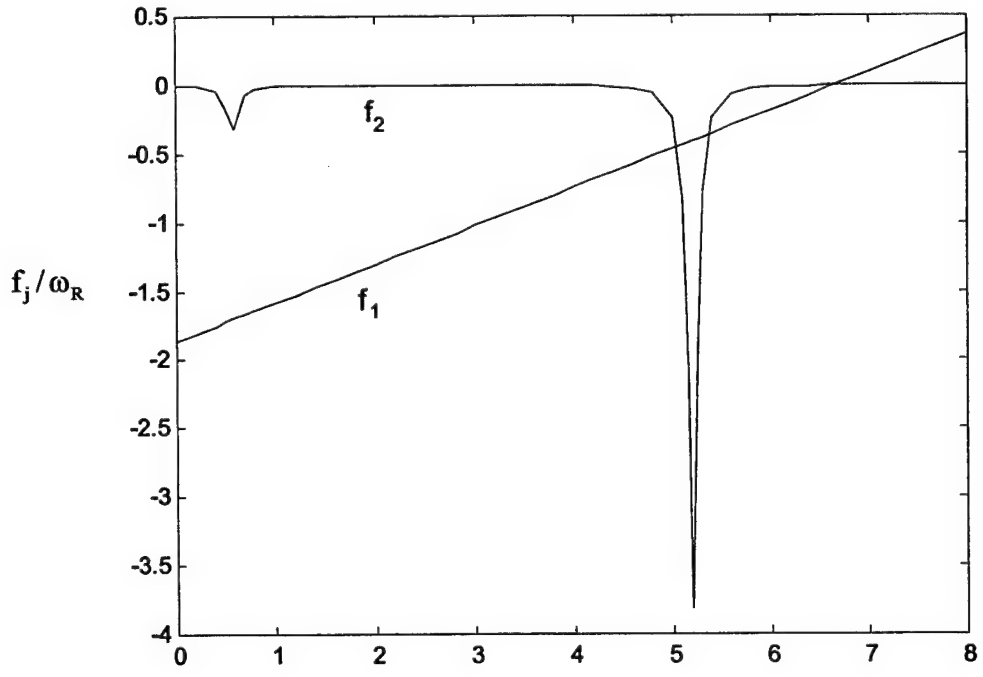

Figure 13. f_j vs. p/ω_R for bent-finned missile at $\sigma = 5$.

Table 1. Values of A_{k0}, N_{k0}, z_{z0}.

k = 1			
σ	A_{k0}	N_{k0}	z_{c0}
5	-3.18 + 30.6i	2082 -14.6i	- 0.64
10	-3.55 + 48.6i	434 -10.5i	- 0.17
20	-3.65 + 52.4i	101 - 3.3i	- 0.04
k = 3			
5	-2.78 + 280i	$(13.1 +3.6i)10^5$	18 + 4.8i
10	-2.44 + 543i	$(3.5 +7.9i)10^6$	12 +27.3i
20	-2.33+1077i	$(1.0 +18.5i)10^6$	0.9 +15.8i
k = 5			
5	-1.34 + 747i	-55729 +10586i	-0.22 –0.02i
10	-1.38+1485i	-53957 +20861i	-0.05-0.008i
20	-1.39+2963i	-53374 +41579i	-0.01-0.004i

13. References

1. Platus, D. H. "Aeroelastic Stability of Slender, Spinning Missiles." *Journal of Guidance, Control, and Dynamics*, vol. 15, pp. 144–151, January/February 1992.

2. Legner, H. H., E. Y. Lo, and W. G. Reinecke. "On the Trajectory of Hypersonic Projectiles Undergoing Geometry Changes." AIAA Aerospace Sciences Meeting, Reno, NV, AIAA 94-0719, 10–13 January 1994.

3. Mikhail, A. G. "In-Flight Flexure and Spin Lock-in for Anti-Tank Kinetic Energy Projectiles." *Journal of Spacecraft and Rockets*, vol. 33, pp. 657–664, September–October 1996.

4. Mikhail, A. G. "In-Flight Flexure and Spin Lock-in for Anti-Tank Kinetic Energy Projectiles." ARL-TR-882, U.S. Army Research Laboratory, Aberdeen Proving Ground, MD, October 1995.

5. Heddadj, S., R. Cayzac, and J. Renard. "Aeroelasticity of High L/D Supersonic Bodies: Theoretical and Numerical Approach." AIAA Aerospace Sciences Meeting, Reno, NV, AIAA 2000–0390, 10–13 January 2000.

6. Murphy, C. H., and W. H. Mermagen. "Flight Mechanics of an Elastic Symmetric Projectile." *Journal of Guidance, Control, and Dynamics*, vol. 24, November–December 2001.

7. Murphy, C. H., and W. H. Mermagen. "Flight Mechanics of an Elastic Symmetric Projectile." ARL-TR-2255, U.S. Army Research Laboratory, Aberdeen Proving Ground, MD, April 2000.

8. Murphy, C. H. "Some Special Cases of Spin-Yaw Lock-In." *Journal of Guidance, Control, and Dynamics*, vol. 12, pp. 771–776, November–December 1989.

9. Murphy, C. H. "Some Special Cases of the Spin-Yaw Lock-In." BRL-MR-3609, U.S. Army Ballistic Research Laboratory, Aberdeen Proving Ground, MD, August 1987.

10. Wood, R. M., and C. H. Murphy. "Aerodynamic Derivatives for Both Steady and Nonsteady Motion of Slender Missiles." *Journal of Aeronautical Science*, vol. 22, pp. 670–571, December 1955.

11. Wood, R. M., and C. H. Murphy. "Aerodynamic Derivatives for Both Steady and Nonsteady Motion of Slender Missiles." BRL-MR-880, U.S. Army Ballistic Research Laboratory, Aberdeen Proving Ground, MD, April 1955.

12. Munk, M. M. "The Aerodynamic Forces on Airship Hulls." NACA-TR-184, 1923.

13. Devan, L., and L. A. Mason. "Aerodynamics of Tactical Weapons to Mach Number 8 and Angle of Attack 180: Part II Computer Program and Users Guide." Naval Surface Weapons Center, Dahlgren, VA, NSWC-TR-81-358, September 1981.

14. Durand, W. F. "Aerodynamic Theory." Reprint ed., Pasadena: California Institute of Technology, pp. 110–112, 1943.

15. Murphy, C. H. "Free Flight Motion of Symmetric Missiles." BRL-MR-1216, U.S. Army Ballistic Research Laboratory, Aberdeen Proving Ground, MD, July 1963.

16 De Silva, C. W. *Vibration: Fundamentals and Practice*. Boca Raton: CRC Press, p. 351, 2000.

17. Géradin, M., and D. Rixen. *Mechanical Vibrations: Theory and Applications to Structural Dynamics*. New York: Wiley & Sons, 1994.

18. Chapman, G. T., and D. B. Kirk. "A New Method for Extracting Aerodynamic Coefficients from Free Flight Data." *AIAA Journal*, vol. 8, pp. 753–758, April 1970.

19. Guidos, B. J., J. M. Garner, J. F. Newill, and C. D. Livecchia. "Measured In-Flight Rod Flexure of a 120-mm M829E3 Kinetic Energy (KE) Projectile Steel Model." U.S. Army Research Laboratory, Aberdeen Proving Ground, MD, to be published.

Appendix A. Integrals

A.1 Aerodynamic Integrals

$$C_{N\alpha} = \int_{x_0}^{x_3} c_{f1}\,dx \qquad C_{M\alpha} = \int_{x_0}^{x_3} c_{f1}\,x\,dx$$

$$C_{Nq} = \int_{x_0}^{x_3} (c_{f2} - x c_{f1})\,dx \qquad C_{Mq} = \int_{x_0}^{x_3} (c_{f2} - x c_{f1})\,x\,dx$$

$$C_{N\dot{\alpha}} = \int_{x_0}^{x_3} c_{f2}\,dx \qquad C_{M\dot{\alpha}} = \int_{x_0}^{x_3} c_{f2}\,x\,dx$$

$$C_{NBF} = \int_{x_0}^{x_3} c_{f1}\Gamma_{BF}\,dx \qquad C_{MBF} = \int_{x_0}^{x_3} c_{f1}\Gamma_{BF}\,x\,dx$$

A.2 Boundary Conditions Integrals

$$I_1 = \int_{x_0}^{x_1} c_{f1}\,dx \qquad I_2 = \int_{x_2}^{x_3} c_{f1}\,dx$$

$$I_3 = \int_{x_0}^{x_1} (x - x_1) c_{f1}\,dx \qquad I_4 = \int_{x_2}^{x_3} (x - x_2) c_{f1}\,dx$$

$$I_5 = \int_{x_0}^{x_1} c_{f2}\,dx \qquad I_6 = \int_{x_2}^{x_3} c_{f2}\,dx$$

$$I_7 = \int_{x_0}^{x_1} (x - x_1) c_{f2}\,dx \qquad I_8 = \int_{x_2}^{x_3} (x - x_2) c_{f2}\,dx$$

$$I_9 = \int_{x_0}^{x_1} (x - x_1)^2 c_{f1}\,dx \qquad I_{10} = \int_{x_2}^{x_3} (x - x_2)^2 c_{f1}\,dx$$

$$I_{11} = 2I_5 - I_3 - x_1 I_1 \qquad I_{12} = 2I_6 - I_4 - x_2 I_2$$

$$I_{13} = 2I_7 - I_9 - x_1 I_3 \qquad I_{14} = 2I_8 - I_{10} - x_2 I_4$$

$$I_{1D} = \int_{x_0}^{x_1} c_D\,dx + c_{Dbp} \qquad I_{2D} = \int_{x_2}^{x_3} c_D\,dx$$

$$I_{3D} = \int_{x_0}^{x_1} (x - x_1) c_D\,dx \qquad I_{4D} = \int_{x_2}^{x_3} (x - x_2) c_D\,dx$$

$$I_{1BF} = \int_{x_0}^{x_1} c_{f1}\Gamma_{BF}\,dx \qquad I_{3BF} = \int_{x_0}^{x_1} (x - x_1) c_{f1}\Gamma_{BF}\,dx$$

INTENTIONALLY LEFT BLANK.

Appendix B. Functions

$$J_1(t) = \int_{x_0}^{x_3} c_{f1}\Gamma dx \qquad J_5(t) = \int_{x_0}^{x_3} c_D \delta dx + \delta(x_1) c_{Dbp}$$

$$J_2(t) = \int_{x_0}^{x_3} (c_{f2}\Gamma - c_{f1}\delta_E) dx \qquad J_6(t) = (1/L)\int_{x_1}^{x_2} x\delta_E dx$$

$$J_3(t) = \int_{x_0}^{x_3} c_{f1}\Gamma x dx \qquad J_7(t) = -(i/L)\int_{x_1}^{x_2} (\dot{\delta}\bar{\delta} + \dot{\Gamma}_m \bar{\Gamma}) dx$$

$$J_4(t) = \int_{x_0}^{x_3} (c_{f2}\Gamma - c_{f1}\delta_E) x dx \qquad J_8(t) = -(1/16L)\int_{x_1}^{x_2} (\dot{\Gamma} - 2ip\Gamma) dx$$

$$J_9(t) = i\int_{x_0}^{x_3} c_{f1}\left[(\xi - \Gamma) + (\dot{\delta}_E - ixQ)(d/V)\right]\bar{\delta} dx$$

$$J_E(t) = -(g_1 d)\left[J_3 + \dot{J}_4(d/V) + J_5\right]$$

$$J_N(t) = \left[I_t \dot{N} - (ipI_x)N\right](d/V)$$

$$\tilde{c}_{dr} = 2\omega_1^{-1}\frac{\partial^r}{\partial x^r}\left(\frac{\partial \tilde{\delta}_E}{\partial t} - ip\tilde{\delta}_E\right)$$

$$N(t) = g_2\left[J_1 + \dot{J}_2(d/V)\right] - \ddot{\delta}_c$$

$$E_1(x) = g_2(C_{N\alpha} - Lc_{f1})$$

$$E_2(x) = g_2(C_{N\dot{\alpha}} + C_{Nq} - Lc_{f3})(d/V)$$

$$E_{BF} = g_2(C_{NBF} - Lc_{f1}\Gamma_{BF})$$

$$c_{f3}(x) = 2c_{f2} - xc_{f1}$$

$$\dot{\Gamma}_m(x,t) = (\dot{\Gamma} - 2ip\Gamma + iQ)/16$$

$$f_1(t) = I_1[\xi(t) - \Gamma(x_1,t)] + \left[I_{11}\dot{\xi}(t) + I_1\dot{\delta}_E(x_1,t) + (I_3 - I_5)\dot{\Gamma}(x_1,t)\right](d/V)$$

$$f_2(t) = I_2[\xi(t) - \Gamma(x_2,t)] + \left[I_{12}\dot{\xi}(t) + I_2\dot{\delta}_E(x_2,t) + (I_4 - I_6)\dot{\Gamma}(x_2,t)\right](d/V)$$

$$m_1(t) = I_3[\xi(t) - \Gamma(x_1,t)] + \left[I_{13}\dot{\xi}(t) + I_3\dot{\delta}_E(x_1,t) + (I_9 - I_7)\dot{\Gamma}(x_1,t)\right](d/V) - m_{1D}$$

$$m_2(t) = I_4[\xi(t) - \Gamma(x_2,t)] + \left[I_{14}\dot{\xi}(t) + I_4\dot{\delta}_E(x_2,t) + (I_{10} - I_8)\dot{\Gamma}(x_2,t)\right](d/V) - m_{2D}$$

$$m_{1D}(t) = I_{1D}[\delta_E(x_1,t) - \delta_c(t)] + I_{3D}\Gamma(x_1,t)$$

$$m_{2D}(t) = I_{2D}[\delta_E(x_2,t) - \delta_c(t)] + I_{4D}\Gamma(x_2,t)$$

INTENTIONALLY LEFT BLANK.

Appendix C. Relationship Between Boundary Conditions

If we make the slender missile assumptions ($I_t \cong md^2L^2/12\,;\, I_x/I_t \cong \dot{I}_8/\ddot{I}_8 \cong 0$), the boundary conditions at x_1 and x_2 are directly related. This can be shown by first integrating equation (51) from x_1 to x at fixed time.

$$\int_{x_1}^{x} \ddot{\delta} dx - i\dot{Q}\left(x^2 - x_1^2\right)/2 - g_2\left[C_{N\alpha}\xi - J_1 + \left[\left(C_{N\dot{\alpha}} + C_{Nq}\right)\dot{\xi} - \dot{J}_2\right](d/V)\right](x - x_1)/L =$$
$$-\omega_0^2\left[\frac{\partial^3 \delta_E(x)}{\partial x^3} - \frac{\partial^3 \delta_E(x_1)}{\partial x^3}\right] - \hat{k}\omega_0^2\left[c_{d3}(x) - c_{d3}(x_1)\right] \qquad \text{(C-1)}$$
$$-g_2\int_{x_1}^{x}\left[c_{f1}(\xi - \Gamma) + \left[c_{f1}\left(\dot{\delta}_E - x\dot{\xi}\right) + c_{f2}\left(2\dot{\xi} - \dot{\Gamma}\right)\right](d/V)\right]dx$$
$$-g_2\left[c_D(x)\delta(x) - c_D(x_1)\delta(x_1)\right].$$

Equation (C-1) is now evaluated at x_2 using the integrals of C.1.

$$\frac{\partial^3 \delta_E(x_2)}{\partial x^3} + \hat{k}c_{d3}(x_2) = \frac{\partial^3 \delta_E(x_1)}{\partial x^3} + \hat{k}c_{d3}(x_1) - g_4\left[c_D(x_2)\delta(x_2) - c_D(x_1)\delta(x_1)\right] \qquad \text{(C-2)}$$
$$+ g_4(f_1 + f_2),$$

where f_j is defined in Appendix B.

According to equation (C-2), boundary condition (53) implies boundary condition (55).

If equation (C-1) is integrated from x_1 to x_2, five single integrals and six double integrals result. Each of the double integrals can be simplified by integration by parts and are given in section C.3.

Under our stated assumptions, equation (36) becomes

$$\left(L^2/12\right)\dot{Q} + i\dot{J}_6 = -ig_2\left[C_{M\alpha}\xi - J_3 + \left(\left(C_{M\dot{\alpha}} + C_{Mq}\right)\dot{\xi} - \dot{J}_4\right)(d/V) - J_5\right]. \qquad \text{(C-3)}$$

Equation (C-1) is now integrated and simplified by use of sections C.1–C.4 and equations (53) and (A-3),

$$\frac{\partial^2 \delta_E(x_2)}{\partial x^2} + \hat{k}c_{d2}(x_2) = \frac{\partial^2 \delta_E(x_1)}{\partial x^2} + \hat{k}c_{d2}(x_1) + g_4(m_1 + m_2), \qquad \text{(C-4)}$$

where m_j is defined in Appendix B.

Boundary condition (54) is equivalent, therefore, to boundary condition (56).

C.1 Integrals in Equation (C-2)

$$\int_{x_1}^{x_2} \ddot{\delta} dx = 0 \qquad \int_{x_1}^{x_2} c_{f1} dx = C_{N\alpha} - I_1 - I_2$$

$$\int_{x_1}^{x_2} c_{f1} \Gamma dx = J_1 - I_1\Gamma_1 - I_2\Gamma_2 \qquad \int_{x_1}^{x_2} c_{f2} dx = C_{N\dot{\alpha}} - I_5 - I_6$$

$$\int_{x_1}^{x_2} (c_{f2} - x c_{f1}) dx = C_{Nq} - (I_{11} - I_5) - (I_{12} - I_6)$$

$$\int_{x_1}^{x_2} (c_{f1}\dot{\delta}_E - c_{f2}\dot{\Gamma}) dx = -\dot{J}_2 - I_1\dot{\delta}_{E1} - (I_3 - I_5)\dot{\Gamma}_1 - I_2\dot{\delta}_{E2} - (I_4 - I_6)\dot{\Gamma}_2$$

C.2 Integrals in Equation (C-4)

$$(1/2)\int_{x_1}^{x_2} (x^2 - x_1^2) dx = -L^3/12 \qquad L^{-1}\int_{x_1}^{x_2} (x - x_1) dx = L/2$$

$$\int_{x_1}^{x_2} \left[\frac{\partial^3 \delta_E(x)}{\partial x^3} - \frac{\partial^3 \delta_E(x_1)}{\partial x^3} \right] dx = \frac{\partial^2 \delta_E(x_2)}{\partial x^2} - \frac{\partial^2 \delta_E(x_1)}{\partial x^2} - \frac{\partial^3 \delta_E(x_1)}{\partial x^3} L$$

$$\int_{x_1}^{x_2} [c_{d3}(x) - c_{d3}(x_1)] dx = c_{d2}(x_2) - c_{d2}(x_1) - c_{d3}(x_1) L$$

$$\int_{x_1}^{x_2} c_D \delta dx = J_5 - I_{3D} - I_{4D}$$

C.3 Multiple Integrals in Equation (C-4)

$$\int_{x_1}^{x_2}\int_{x_1}^{x} \ddot{\delta} dx\, dx = -L\ddot{J}_6$$

$$\int_{x_1}^{x_2}\int_{x_1}^{x} c_{f1} dx\, dx = L[(1/2)C_{N\alpha} - I_1] - [C_{M\alpha} - I_3 - I_4]$$

$$\int_{x_1}^{x_2}\int_{x_1}^{x} c_{f1}\Gamma dx\, dx = L[(1/2)J_1 - I_1\Gamma_1] - [J_3 - I_3\Gamma_1 - I_4\Gamma_2]$$

$$\int_{x_1}^{x_2}\int_{x_1}^{x} c_{f2} dx\, dx = L[(1/2)C_{N\dot{\alpha}} - I_5] - (C_{M\dot{\alpha}} - I_7 - I_8)$$

$$\int_{x_1}^{x_2}\int_{x_1}^{x}(c_{f2}-xc_{f1})dx\,dx = L\left[(1/2)C_{Nq}-(I_{11}-I_5)\right]-\left[C_{Mq}-(I_{13}-I_7)-(I_{14}-I_8)\right]$$

$$\int_{x_1}^{x_2}\int_{x_1}^{x}(c_{f1}\dot{\delta}_E-c_{f2}\dot{\Gamma})dx\,dx = L\left[-(1/2)\dot{J}_2-I_1\dot{\delta}_{E1}-(I_3-I_5)\dot{\Gamma}_1\right]$$

$$-\left[-\dot{J}_4-I_3\dot{\delta}_{E1}-(I_9-I_7)\dot{\Gamma}_1-I_4\dot{\delta}_{E2}-(I_{10}-I_8)\dot{\Gamma}_2\right]$$

INTENTIONALLY LEFT BLANK.

Appendix D. Trim Solution Parameters

$$b_1 = a_1 + ip(a_2 + a_3) - p^2(I_t - I_x)$$

$$J_{ET} = -(g_1 d)[J_{3T} + J_{5T} + i(pd/V)J_{4T}]$$

$$J_{NT} = i(I_t - I_x)(pd/V)N_T$$

$$J_{BF} = ig_2(I_t - I_x)(pd/V)C_{NBF}$$

$$N_T = g_2[J_{1T} + J_{2T}(ipd/V)] + p^2\delta_{cT}$$

J_{jT} for j = 1,2,3,4,5,6 is J_j with δ_E, Γ replaced by δ_{ET}, Γ_T

$$E_{2L} = E_2 + g_2(xd/V)C_{L\alpha}$$

$$E_3 = (E_1 + ipE_{2L} - p^2 x)/\omega_0^2$$

$$E_4 = g_4[c_{f1} + (ipd/V)c_{f2} - c_D]$$

$$E_5 = -p^2/\omega_0^2 + g_4\left[c_{f1}(ipd/V) + \frac{dc_D}{dx}\right]$$

$$\tilde{\delta}_{cT} = (1/L)\int_{x_1}^{x_2} \tilde{\delta}_{ET} dx$$

$$N_T^* = [1 + ix(pd/V)]N_T\omega_0^{-2}$$

$$E_{BF}^* = [E_{BF} + ix(p\,d/V)C_{NBF}]\omega_0^{-2}$$

$$E_B = g_4\left[c_{f1}\Gamma_B + (c_{f2}\Gamma_B - c_{f1}\delta_{EB})(ipd/V) - \frac{d(c_D\delta_B)}{dx}\right] + (p/\omega_0)^2\delta_B$$

$$f_{1T} = I_1(\xi_T - \Gamma_T(x_1)) + [I_{11}\xi_T + I_1\delta_{ET}(x_1) + (I_3 - I_5)\Gamma_T(x_1)](ipd/V) - I_{1BF}$$

$$f_{2T} = I_2(\xi_T - \Gamma_T(x_1)) + [I_{12}\xi_T + I_2\delta_{ET}(x_2) + (I_4 - I_6)\Gamma_T(x_1)](ipd/V)$$

$$m_{1T} = I_3(\xi_T - \Gamma_T(x_1)) + [I_{13}\xi_T + I_3\delta_{ET}(x_1) + (I_9 - I_7)\Gamma_T(x_1)](ip/V) - m_{1DT} - I_{3BF}$$

$$m_{2T} = I_4(\xi_T - \Gamma_T(x_1)) + [I_{14}\xi_T + I_4\delta_{ET}(x_2) + (I_{10} - I_8)\Gamma_T(x_1)](ipd/V) - m_{2DT}$$

$$m_{1DT} = I_{1D}[\delta_{ET}(x_1) - \delta_{Tc}] + I_{3D}\Gamma_T(x_1)$$

$$m_{2DT} = I_{2D}[\delta_{ET}(x_2) - \delta_{Tc}] + I_{4D}\Gamma_T(x_2)$$

INTENTIONALLY LEFT BLANK.

Appendix E. Transient Solution Parameters

$$b_{1k} = a_1 + ipa_3 + (a_2 - ipI_x)A_k + I_t A_k^2$$

$$J_{Ek} = -(g_1 d)[J_{3k} + J_{5k} + (A_k d/V)J_{4k}]$$

$$J_{Nk} = (A_k I_t - ipI_x)(d/V)N_k$$

$$N_k = g_2[J_{1k} + J_{2k}(A_k d/V)] - A_k^2 \psi_{kc}$$

J_{jk} for $j = 1,2,3,4,5,6$ is J_j with δ_E, Γ replaced by $\psi_k, \dfrac{d\psi_k}{dx}$

$$E_{3k} = (E_1 + A_k E_{2L} + A_k^2 x)\omega_0^{-2}$$

$$E_{4k} = g_4[c_{f1} + (A_k d/V)c_{f2} - c_D]$$

$$E_{5k} = A_k^2/\omega_0^2 + g_4\left[c_{f1}(A_k d/V) + \frac{dc_D}{dx}\right]$$

$$E_{6k} = 1 + 2\hat{k}\omega_1^{-1}(A_k - ip)$$

$$\psi_{kc} = (1/L)\int_{x_1}^{x_2} \psi_k dx$$

$$N_k^* = [1 + x(A_k d/V)]N_k \omega_0^{-2}$$

$$f_{1k} = I_1\left(1 - \frac{d\psi_k(x_1)}{dx}\right) + \left[I_{11} + I_1\psi_k(x_1) + (I_3 - I_5)\frac{d\psi_k(x_1)}{dx}\right](A_k d/V)$$

$$f_{2k} = I_2\left(1 - \frac{d\psi_k(x_2)}{dx}\right) + \left[I_{12} + I_2\psi_k(x_2) + (I_4 - I_6)\frac{d\psi_k(x_2)}{dx}\right](A_k d/V)$$

$$m_{1k} = I_3\left(1 - \frac{d\psi_k(x_1)}{dx}\right) + \left[I_{13} + I_3\psi_k(x_1) + (I_9 - I_7)\frac{d\psi_k(x_1)}{dx}\right](A_k d/V) - m_{1Dk}$$

$$m_{2k} = I_4\left(1 - \frac{d\psi_k(x_2)}{dx}\right) + \left[I_{14} + I_4\psi_k(x_2) + (I_{10} - I_8)\frac{d\psi_k(x_2)}{dx}\right](A_k d/V) - m_{2Dk}$$

$$m_{1Dk} = I_{1D}[\psi_k(x_1) - \psi_{kc}] + I_{3D}\frac{d\psi_k(x_1)}{dx}$$

$$m_{2Dk} = I_{2D}[\psi_k(x_2) - \psi_{kc}] + I_{4D}\frac{d\psi_k(x_2)}{dx}$$

INTENTIONALLY LEFT BLANK.

Appendix F. Missile Parameters

F.1 Flare-Stabilized Missile Parameters

$L = 25$

$d = 0.20\,\text{ft}$

$m = 2.40\,\text{slug}$

$I_x = 0.0132\,\text{slug}-\text{ft}^2$ (0)

$I_t = 5.006\,\text{slug}-\text{ft}^2$ (5.000)

$c_{f1} = 0$

$= -1.14(x+5)$

$c_{f2} = 0$

$C_{N\alpha} = 32$

$d_{flare} = 0.80\,\text{ft}$

$S = (\pi/4)(d)^2$

$V = 18000\,\text{ft/sec}$

$\rho = .002\,\text{slug/ft}^2$

$-5 < x \le 12.5$

$-12.5 \le x \le -5$

$C_{M\alpha} = -320$

F.2 Finned Missile Parameters

L= 20

d = 0.35 ft.

m = 3.50 slug

I_x = 0.054 slug-ft² (0)

I_t = 14.318 slug-ft² (14.292)

$c_{f1} = 4(11-x)$ $\quad 10 < x \le 11$

$= 4e^{7(x-10)}$ $\quad -5 < x \le 10$

$= -(2/\pi)(15+3x)a_L$ $\quad -7 < x \le -5$

$= (12/\pi)a_L$ $\quad -11 \le x \le -7$

$c_{f2} = 2(11-x)^2$ $\quad 10 < x \le 11$

$= 2 + 0.571(1-e^{7(x-10)})$ $\quad -5 < x \le 10$

$= 2.571 + (1/3\pi)(15+3x)^2 a_L$ $\quad -7 < x \le -5$

$= 2.571 - (12/\pi)(6+x)a_L$ $\quad -11 \le x \le -7$

$c_D = (0.30)(11-x) - 0.295e^{-10(x-10)}$ $\quad 10 < x \le 11$

$= 0.0050$ $\quad -5 < x \le 10$

$= -0.10(5+x) + 0.005 - 0.198e^{10(x+7)}$ $\quad -7 < x \le -5$

$= 0.0070$ $\quad -11 \le x \le -7$

$c_{Dbp} = 0.14$ $\quad C_{tp} = -18$

V = 6000 ft/s

ρ = 0.002 slugs/ft³

$x_{01} = x_{23} = 1$

a_s = 1100 ft/s

$a_L = 2\left[\sqrt{(V/a_s)^2 - 1}\right]^{-1}$

$d_{12} = 10^{-3}$ $\quad$ $d_{22} = -0.25x10^{-5}$

$C_{N\alpha} = 9.7$ $\quad$ $C_{M\alpha} = -34.4$

$C_{Mq} = -980$ $\quad$ $C_{M\dot{\alpha}} = -190$

List of Symbols

A (x)	local cross-sectional area
$c_{fj}(x)$	aerodynamic force distributions functions
d	rod diameter
E	Young's modulus
$\hat{F}_a$	complex aerodynamic shear force on rod at x
$\hat{F}_d$	complex beam damping shear force on rod at x
$\hat{F}_e$	complex beam elastic shear force on beam at x
g_1	$\rho V^2 S/2$
g_2	g_1/md
g_3	$\rho VSd/2m$
g_4	$g_2 L/\omega_0^2$
g_x	I_x/md^2
g_t	I_t/md^2
I	$(d)^4 \iint y^2 dydz = (d)^4 \iint z^2 dydz$, area moment of rod
I_x	axial moment of inertia of projectile
I_t	transverse moment of inertia of projectile
$\hat{k}$	beam-damping coefficient
L	dimensionless length of rod
m	projectile mass
M_e	complex elastic moment on rod at x
p	projectile spin
Q	$q + ir$, complex transverse angular velocity of body 1
S	$\pi d^2/4$

V	magnitude of projectile velocity
x_1, x_2	location of beam ends
x_{01}, x_{23}	dimensionless length of fore and aft aerodynamic extensions
α	angle of attack of central disk
β	angle of sideslip of central disk
Γ	$\frac{\partial \delta}{\partial x}$, cant of disk
δ	$\delta_E - \delta_c$ lateral displacement of disk relative to missile center of mass (cm)
δ_c	$L^{-1}\int_{x_1}^{x_2}\delta_E dx$, lateral location of missile's cm
δ_E	$\delta_{Ey} + i\delta_{Ez}$, lateral displacement of disk relative to central disk
ϕ	roll angle
$\dot{\phi}_k$	frequency of k-th mode
λ_k	damping of k-th mode
η	complex angle of attack of disk
ρ	air density
ρ_1	m/Ld, linear density of rod
σ	ω_1/ω_R
ω_0^2	$EI/\rho_1 d^4$
ω_1	lowest elastic frequency of beam in vacuum
ω_R	rigid projectile zero-spin frequency
ξ	$\beta + i\alpha$, complex angle of attack of projectile
$\vec{F} = (F_x, F_y, F_z)$	aerodynamic force exerted on missile
$\vec{H} = (H_x, H_y, H_z)$	angular momentum of missile

$\vec{M} = (M_x, M_y, M_z)$ aerodynamic moment exerted on missile

$\vec{V} = (v_x, v_y, v_z)$ missile velocity

$\vec{V}_{dc} = (v_x, v_{dcy}, v_{dcz})$ velocity of disk relative to missile's cm

$\vec{\delta}_E = (x, \delta_{Ey}, \delta_{Ez})$ dimensionless location of disk relative to central disk

$\vec{\delta} = (x, \delta_y, \delta_z)$ dimensionless location of disk relative to missile's cm

$\vec{\omega} = (p,q,r)$ angular velocity of central disk

$\vec{\Omega} = (0,q,r)$ angular velocity of non-spinning elastic coordinates

$R\{z\}$ real part of z

$I\{z\}$ imaginary part of z

Circumflex superscript denotes a beam shear force

Tilde superscript denotes elastic parameter for bent missile

B subscript denotes parameter for bent projectile

BF subscript denotes bent fin parameter

E subscript denotes elastic coordinates at central disk

T subscript denotes trim motion parameter

INTENTIONALLY LEFT BLANK.

REPORT DOCUMENTATION PAGE

Form Approved
OMB No. 0704-0188

1. AGENCY USE ONLY *(Leave blank)*	2. REPORT DATE	3. REPORT TYPE AND DATES COVERED
	June 2002	Final, November 2000–November 2001

4. TITLE AND SUBTITLE
Flight Motion of a Continuously Elastic Finned Missile

5. FUNDING NUMBERS
AH80

6. AUTHOR(S)
Charles H. Murphy and William H. Mermagen

7. PERFORMING ORGANIZATION NAME(S) AND ADDRESS(ES)
U.S. Army Research Laboratory
ATTN: AMSRL-WM-MC
Aberdeen Proving Ground , MD 21005-5069

8. PERFORMING ORGANIZATION REPORT NUMBER
ARL-TR-2754

9. SPONSORING/MONITORING AGENCY NAMES(S) AND ADDRESS(ES)

10.SPONSORING/MONITORING AGENCY REPORT NUMBER

11. SUPPLEMENTARY NOTES

12a. DISTRIBUTION/AVAILABILITY STATEMENT
Approved for public release; distribution is unlimited.

12b. DISTRIBUTION CODE

13. ABSTRACT*(Maximum 200 words)*

The motion of elastic finned projectiles has been analyzed by various approximate theories. In this report the exact equations of small amplitude motion are derived for a symmetric missile. The aerodynamic and elastic symmetries are used to allow the use of complex variables to describe the lateral motion in a non-rotating coordinate system. Although the resulting equations are both ordinary and partial differential equations, frequencies and damping rates of free oscillations are obtained from an ordinary differential equation with boundary conditions. Equations for a permanently deformed bent missile are derived, and an ordinary differential equation for the forced motion of a bent missile is obtained. Sample calculations for a finned projectile with a fineness ratio of 20 show resonant motion at the aerodynamic frequency as well as at each elastic frequency. The nonlinear roll moment associated with a bent missile is computed and the location of possible spin-yaw lock-in is determined. The flight motion of an elastic missile is shown to be the sum of two elliptical motions: a low frequency pitching motion and a higher frequency flexing motion. The induced drag coefficients for both motions are computed as functions of the missile's elasticity.

14. SUBJECT TERMS
flight mechanics, elastic missile, spin-yaw lock-in, aeroelastic motion

15. NUMBER OF PAGES
53

16. PRICE CODE

17. SECURITY CLASSIFICATION OF REPORT	18. SECURITY CLASSIFICATION OF THIS PAGE	19. SECURITY CLASSIFICATION OF ABSTRACT	20. LIMITATION OF ABSTRACT
UNCLASSIFIED	UNCLASSIFIED	UNCLASSIFIED	UL

INTENTIONALLY LEFT BLANK.